
Targeted Reduction of Causal Models

Armin Kekić

Bernhard Schölkopf

Michel Besserve

Max Planck Institute for Intelligent Systems, Tübingen, Germany

Abstract

Why does a phenomenon occur? Addressing this question is central to most scientific inquiries based on empirical observations, and often heavily relies on simulations of scientific models. As models become more intricate, deciphering the causes behind these phenomena in high-dimensional spaces of interconnected variables becomes increasingly challenging. Causal machine learning may assist scientists in the discovery of relevant and interpretable patterns of causation in simulations. We introduce *Targeted Causal Reduction* (TCR), a method for turning complex models into a concise set of causal factors that explain a specific target phenomenon. We derive an information theoretic objective to learn TCR from interventional data or simulations and propose algorithms to optimize this objective efficiently. TCR’s ability to generate interpretable high-level explanations from complex models is demonstrated on toy and mechanical systems, illustrating its potential to assist scientists in the study of complex phenomena in a broad range of disciplines.

1 INTRODUCTION

Mathematical models are crucial in science for representing real-world systems and serve various purposes, including generating *etiological explanations*—identifying the causes of specific phenomena. For instance, general circulation models address the causes of global warming (Grassl, 2000), while computational models of the brain investigate the origins of pathologies (Breakspear, 2017; Deco and Kringelbach, 2014). These examples illustrate the increasing complexity of scientific models, designed to faithfully capture the large number of mechanisms at play in these systems. However, this complexity comes at a

cost: expanding parameter spaces and heightened computational demands. This trend, in turn, impacts the ability to generate high-level explanations, understandable by scientists and decision makers (Reichstein et al., 2019; Safavi et al., 2023). This is analogous to challenges of explainable AI: explaining a system can be difficult even when its mechanisms are perfectly known.

Consider the system of point masses depicted in Fig. 1a. Its trajectory can be accurately predicted by simulating the coupled equations of motion of individual point masses. Suppose, we are interested in one property of this system’s trajectory that takes the form of one single scalar variable Y , that we call the *target variable*. Let us take Y to be the horizontal speed of the system’s center of gravity. We would like to discover its “causes”, meaning which properties of the system influence Y and the mechanisms mediating this influence. In principle, it is possible to derive these from this “microscopic” model. However, this set is large as it includes all internal and external forces exerted on individual points. In contrast, the horizontal motion of the center of gravity can be described by a single scalar differential equation, subject to a single *net force*—the sum of all horizontal components of external forces.

This illustrates the goal we want to achieve, depicted in Fig. 1b. Starting from a complex *low-level model* described by a vector of variables \mathbf{X} and a target scalar variable Y derived from it (such that $Y = \tau_0(\mathbf{X})$, for some function τ_0), we want to learn a transformation that maps \mathbf{X} to fewer variables forming a *high-level model*. This high-level model should capture the causal influences on Y in a concise and interpretable way, while remaining *consistent* with the low-level model. This notion of consistency is defined using *structural causal models* (SCM) (Pearl, 2009) and interventions on them. The variables of a low-level SCM are mapped to variables of a high-level SCM through a transformation τ , while low-level interventions are correspondingly mapped to high-level interventions through another transformation ω .

Ideally, transformations should satisfy the equivalence of the following two paths: (1) intervening on the low-level model and mapping the outcome to the high-level

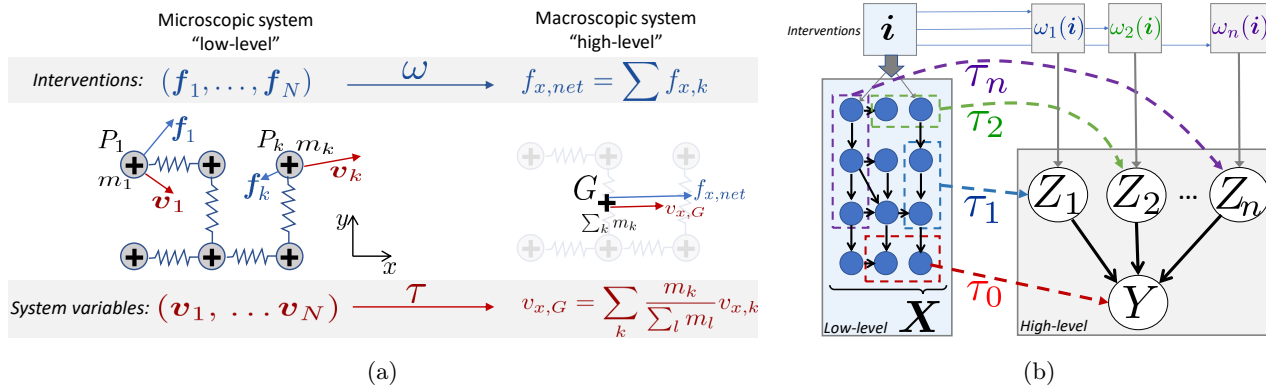


Figure 1: **Targeted Causal Reduction.** (a) Example targeted model reduction: a model of the dynamics of a system of point masses can be reduced to the trajectory of its center of gravity. (b) Principle of TCR.

with τ , or (2) first mapping the low-level model to the high-level model with τ and then applying the high-level intervention derived from the low-level one using ω . A transformation between models satisfying such a *consistency* constraint is called *exact* (Rubenstein et al., 2017; Beckers and Halpern, 2019). However, in practice, one may only be able to achieve it approximately (Beckers et al., 2020).

In this work, we use the Kullback-Leibler divergence to formulate the above *interventional consistency* constraint as a learning objective. Starting from a set of interventional distributions of a given low-level SCM with target variable Y , we learn the transformation and the high-level SCM that form a causal explanation for Y . We propose the *Targeted Causal Reduction* algorithm to minimize the consistency objective by stochastic gradient descent and apply it to synthetic and scientific models to demonstrate our approach.

2 BACKGROUND

2.1 Structural causal models

Causal dependencies between multiple variables can be described using *Structural Causal Models* (SCM) (Peters et al., 2017).

Definition 2.1 (SCM). *An n -dimensional structural causal model is a triplet $\mathcal{M} = (\mathcal{G}, \mathbb{S}, P_U)$ consisting of:*

- a directed acyclic graph \mathcal{G} with n vertices,
- a set $\mathbb{S} = \{X_j := f_j(\mathbf{Pa}_j, U_j), j = 1, \dots, n\}$ of structural equations, where \mathbf{Pa}_j are the variables indexed by the set of parents of vertex j in \mathcal{G} ,
- a joint distribution P_U over the exogenous variables $\{U_j\}_{j \leq n}$, assumed jointly independent.

For each value of the exogenous variables, \mathbb{S} leads to a unique solution for the vector of so-called endogenous variables $\mathbf{X} = [X_1, \dots, X_n]^\top$, such that the distribution

P_U entails a well-defined joint distribution over the endogenous variables $P(\mathbf{X})$. Interventions in SCMs involve replacing one or more structural equations, potentially modifying exogenous distributions, and adding or removing arrows in the original graph to reflect changes in dependencies between variables. An intervention transforms the original model $\mathcal{M} = (\mathcal{G}, \mathbb{S}, P_U)$ into an intervened model $\mathcal{M}^{(i)} = (\mathcal{G}^{(i)}, \mathbb{S}^{(i)}, P_U^{(i)})$, where \mathbf{i} is the vector parameterizing the intervention. The base probability distribution of the unintervened model is denoted $P_M^{(0)}(\mathbf{X})$ or simply $P_M(\mathbf{X})$ and the interventional distribution associated with $\mathcal{M}^{(i)}$ is denoted $P_M^{(i)}(\mathbf{X})$. When there is no ambiguity, we drop the subscript of the base model \mathcal{M} .

While standard *do*-interventions set a structural equation to a constant, they may not correspond to plausible changes of the real-world system being modeled. Instead, *soft interventions* modify an equation while keeping the set of parents unchanged. Large classes of soft interventions can be designed to match domain knowledge (Besserve and Schölkopf, 2022). Notably, the class of *shift interventions* modify the structural equation of endogenous variable l through shifting it by a scalar parameter i

$$\{X_l := f_l(\mathbf{Pa}_l, U_l)\} \mapsto \{X_l := f_l(\mathbf{Pa}_l, U_l) + i\}. \quad (1)$$

These can be combined to form multi-node interventions with vector parameter \mathbf{i} .

2.2 Scientific models and simulations

We use the term *scientific model* to refer to a generative model that relies on a set of equations to represent a phenomenon. What distinguishes such models from generative models in machine learning is their decomposability into elementary functions within parametric classes, encoding domain-specific knowledge about the mechanisms being investigated. We argue that simu-

lators of scientific models can often be expressed as SCMs. This notably includes Ordinary (ODE) and Stochastic Differential Equations (SDE), whose simulation on a discretized grid is performed through explicit numerical schemes. For example, let F be a smooth scalar function and W the standard Brownian motion, the SDE with initial value $X(0) = x_0$ and dynamics

$$dX = F(X(t))dt + \sigma_W \cdot dW,$$

can be simulated over a grid of fixed time step Δt using the Euler–Maruyama method (Sauer, 2013), leading to approximate values $X_k \approx X(k\Delta t)$ following the scheme

$$\begin{cases} X_1 := x_0 + \Delta t \cdot F(x_0) + U_1 \\ X_{k+1} := X_k + \Delta t \cdot F(X_k) + U_{k+1}, \quad k > 1, \end{cases}$$

where $\{U_k\}$ are independent Gaussian variables (see App. A.1 for more details). These sets of equations, spanning all time points, can thus be viewed as a valid SCM with a (linear) DAG structure. Generalization of this view to multidimensional ODE/SDEs as well as Partial Differential Equations is possible (see App. A.1 for more details). Soft interventions on such models, such as shift interventions, can be conceived as modeling perturbations of the real-world system. See App. A.2 for an example system of point masses.

A simulator can thus be seen as a low-level causal model, from which samples of unintervened and intervened distributions can be queried. Those samples will be used to learn a reduction to a high-level causal model.

2.3 Causal Model Reductions (CMR)

We consider as CMR any (possibly approximate) mapping from a low-level SCM \mathcal{L} to a simpler high-level SCM \mathcal{H} . An example is Causal Feature Learning (CFL) (Chalupka et al., 2014, 2016), which achieves a CMR by merging values of a large observation space to yield discrete high-level variables taking values in a small finite set. Consider:

- \mathcal{L} has vector of endogenous variables \mathbf{X} with range \mathcal{X} and set of interventions \mathcal{I} ,
- \mathcal{H} has vector of endogenous variables \mathbf{Z} with range \mathcal{Z} and set of interventions \mathcal{J} .

Starting from the distribution of the low-level model $P_{\mathcal{L}}(\mathbf{X})$, a deterministic mapping $\tau : \mathcal{X} \rightarrow \mathcal{Z}$ generates a joint distribution on the high-level variables that is the push-forward distribution of $P_{\mathcal{L}}(\mathbf{X})$ by τ , denoted $\tau_{\#}[P_{\mathcal{L}}(\mathbf{X})]$ such that

$$\tau(\mathbf{X}) \sim \tau_{\#}[P_{\mathcal{L}}(\mathbf{X})].$$

The low-level interventional distributions can be pushed forward to the high-level in the same way.

A general framework for CMR is based on the notion of *exact transformation* (Rubenstein et al., 2017), which ensures interventional equivalence by matching the pushed forward low-level distributions to the high-level ones.

Definition 2.2 (Exact transformation (Rubenstein et al., 2017)). *A map $\tau : \mathcal{X} \rightarrow \mathcal{Z}$ is an exact transformation from \mathcal{L} to \mathcal{H} if it is surjective, and there exists a surjective map $\omega : \mathcal{I} \rightarrow \mathcal{J}$ such that for all $i \in \mathcal{I}$*

$$\tau_{\#}[P_{\mathcal{L}}^{(i)}(\mathbf{X})] = P_{\mathcal{H}}^{(\omega(i))}(\mathbf{Z}).$$

The set of possible τ can be restricted to *constructive transformations*, which offer good interpretability and come with characterization results (Beckers and Halpern, 2019; Geiger et al., 2023a).

Definition 2.3. *$\tau : \mathcal{X} \rightarrow \mathcal{Z}$ is a constructive transformation between model \mathcal{L} and \mathcal{H} if there exists an alignment map π relating indices of each high-level endogenous variable to a subset of indices of low-level endogenous variables such that for all $k \neq l$, $\pi(k) \cap \pi(l) = \emptyset$ and for each component τ_k of τ it exists a function $\bar{\tau}_k$ such that for all \mathbf{x} in \mathcal{X} ,*

$$\tau_k(\mathbf{x}) = \bar{\tau}_k(\mathbf{x}_{\pi(k)}),$$

i.e. each high-level variable Z_k depends only on the subset of low-level variables given by $\pi(k)$.

The definition of a constructive transformation extends naturally to the intervention map ω , for which we also require that interventions acting on high-level variable k depend only on low-level interventions acting on variables in $\pi(k)$ (see App. A).

Reduction of a scientific model: illustration in mechanics. We illustrate how CMR links to reduction of a scientific model using the above example of Fig. 1a. Consider a system of points $\{\vec{O}P_k = (x_k, y_k)\}$ in a two-dimensional Galilean coordinate system (O, \vec{i}, \vec{j}) . If we are only interested in the position and speed of the system’s center of mass G along the x -axis, the transformation to the high-level model is $\tau_1 : (x_1, y_1, x_2, \dots, v_{x,1}, \dots) \mapsto \frac{1}{\sum_k m_k} \sum_k m_k x_k$ and $\tau_2 : (x_1, y_1, x_2, \dots, v_{x,1}, \dots) \mapsto \frac{1}{\sum_k m_k} \sum_k m_k v_{x,k}$. Moreover, low-level interventions involving forces applied to each point mass solely affect the trajectory of the center of mass through the x component of the *net force*, computed as the sum of all elementary forces, which corresponds to the mapping ω (see Fig. 1a). While there is no SCM associated to this system in the usual sense, there is one associated to the Euler numerical scheme simulating it (see App. A).

3 THEORETICAL ANALYSIS

As described in Fig. 1b, we consider endogenous variables of a low-level model gathered in a (high-dimensional) random vector \mathbf{X} . A target scalar variable $Y = \tau_0(\mathbf{X})$ quantifies a property of interest of this model, and can be thought of as quantifying the presence or magnitude of a *pattern* or *phenomenon* in the data, using *detector* τ_0 . To generate a high-level causal explanation of this pattern, we learn a high-level SCM with fixed effect variable Y and n causes of Y represented by a low-dimensional vector \mathbf{Z} , leading to a high-level (Markovian) causal graph \mathcal{G}_H with only arrows pointing from each Z_k root node to leaf node Y . The low-level variables \mathbf{X} are approximately mapped to the high-level one using a constructive transformation with alignment π . Approximate interventional consistency between models is obtained by defining a mapping ω between interventions at the low level, and their high-level counterpart.

3.1 TCR framework

Our reduction framework has the following elements:

(1) A low-level SCM \mathcal{L} with N endogenous variables $\{X_1, X_2, \dots, X_N\}$ and corresponding exogenous variables $\{U_k\}_{k=1..N}$ equipped with joint distribution $P(\mathbf{U})$. A set of low-level interventions parameterized by vector $\mathbf{i} \in \mathcal{I}$ with distribution $P(\mathbf{i})$, with each component i_k affecting a unique endogenous variable X_k . Unintervened variables are assigned a fixed intervention parameter $i_k = 0$. We only assume we can query (samples from) unintervened and interventional distributions of \mathcal{L} .

(2) A class of high-level SCMs $\{\mathcal{H}_\gamma\}_{\gamma \in \Gamma}$ with $(n+1)$ endogenous variables $\{Y, Z_1, \dots, Z_n\}$ and associated exogenous variables $\{R_k\}_{k=0..n}$, equipped with a factorized distribution $P(\mathbf{R}) = \prod P_{R_k}$. A set of high-level interventions parametrized by vector $\mathbf{j} \in \mathcal{J}$, with each component j_k affecting a single node Z_k . Contrary to the (fixed) low-level model, the high-level model parameters γ need to be learned.

These two models are linked by a constructive transformation with two deterministic surjective maps τ and ω from low- to high-level endogenous variables and interventions, respectively, which decompose as

$$\tau = (\tau_0, \tau_1, \tau_2, \dots, \tau_n) \text{ with } \tau_k : x \mapsto \bar{\tau}_k(x_{\pi(k)}) \quad (2)$$

$$\omega = (\omega_0, \omega_1, \omega_2, \dots, \omega_n) \text{ with } \omega_k : \mathbf{i} \mapsto \bar{\omega}_k(\mathbf{i}_{\pi(k)}) \quad (3)$$

where π is a so-called alignment function from $[0..n]$ to non-overlapping subsets of $[1..N]$. Importantly, τ_0 (and thus $(\bar{\tau}_0, \pi(0))$) are assumed fixed and known. Additionally, ω_0 is assumed to be a trivial constant map $\mathbf{i} \rightarrow 0$, to ensure that the high-level target variable cannot be directly intervened upon, as we want to

explain the changes in Y exclusively through changes of its high-level causes.

The high-level model involves the following mechanisms which need to be learned: (1) The marginal distribution of each high-level cause $P^{(j)}(Z_k)$, in all high-level interventional settings \mathbf{j} . (2) The mechanism $P(Y|\mathbf{Z})$ mapping high-level causes to Y , comprised of the distribution of the exogenous variable R_0 and the map

$$(\mathbf{Z}_1, \dots, \mathbf{Z}_n, R_0) \mapsto f_\gamma(\mathbf{Z}_1, \dots, \mathbf{Z}_n, R_0) =: Y.$$

3.2 Causal consistency loss

It is not always possible (nor desirable) to achieve an exact transformation that guarantees consistency of low- and high-level models for almost all interventions. As a consequence, we allow for the consistency between models to be approximate. To ensure that this approximation is as accurate as possible, we minimize the expected KL divergence between the pushforward by the transformation τ of the low-level interventional distributions that we denote $\widehat{P}_\tau^{(i)}(Y, \mathbf{Z}) = \tau_{\#}[P_{\mathcal{L}}^{(i)}(\mathbf{X})]$, and the corresponding interventional distribution of the high-level model $P^{(\omega(i))}$. The associated consistency loss to be minimized is

$$\mathcal{L}_{cons} = \mathbb{E}_{\mathbf{i} \sim P(\mathbf{i})} \left[KL \left(\widehat{P}_\tau^{(i)}(Y, \mathbf{Z}) \parallel P^{(\omega(i))}(Y, \mathbf{Z}) \right) \right], \quad (4)$$

and has the following properties:

Proposition 3.1 (Consistency loss). *The consistency loss is positive, invariant to invertible reparametrizations, and vanishes if and only if the transformation is exact for almost all interventions. It admits the following decomposition:*

$$\begin{aligned} \mathcal{L}_{cons} = & \mathbb{E}_{\mathbf{i} \sim P(\mathbf{i})} \left[KL \left(\widehat{P}_\tau^{(i)}(\mathbf{Z}) \parallel P^{(\omega(i))}(\mathbf{Z}) \right) \right. \\ & \left. + \mathbb{E}_{\mathbf{z} \sim \widehat{P}_\tau^{(i)}(\mathbf{Z})} \left[KL \left(\widehat{P}_\tau^{(i)}(Y|\mathbf{z}) \parallel P^{(0)}(Y|\mathbf{z}) \right) \right] \right], \quad (5) \end{aligned}$$

and is an upper bound of the causal relevance loss

$$\mathcal{L}_{rel} = \mathbb{E}_{\mathbf{i} \sim P(\mathbf{i})} \left[KL \left(\widehat{P}^{(i)}(Y) \parallel P^{(\omega(i))}(Y) \right) \right] \leq \mathcal{L}_{cons}. \quad (6)$$

The property of reparametrization invariance, detailed in the proof in App. B, refers to transformations of the pairs (τ, f_γ) that leave the composition $f_\gamma \circ \tau$ invariant. In the $n = 1$ linear setting (see Sec. 3.3), this corresponds to invariance by multiplicative rescaling.

We call Eq. (5) a *Cause-Mechanism Decomposition* because the first term quantifies the *cause consistency* and the second term can be thought of as the *mechanism consistency*. This latter term assesses

the similarity between the outputs of the learned high-level mechanism $P^{(0)}(Y|z)$ and the corresponding conditional distribution computed by push-forward of the low-level variables $\widehat{P}_\tau^{(i)}(Y|z)$. Since we prevent the high-level mechanism from being intervened on, only its unintervened conditional appears in the expression.

Lastly, the causal relevance loss \mathcal{L}_{rel} assesses whether the variations of the target Y due to low-level interventions are well captured by high-level interventions, on average over the prior $P(\mathbf{i})$. Its upper bound by \mathcal{L}_{cons} ensures that by optimizing for consistency, we also indirectly promote effective “explanation” of the variations in the target density resulting from low-level interventions. We can thus choose $P(\mathbf{i})$ to make the most relevant interventions more likely according to domain knowledge, such that optimizing the loss will steer towards a solution capturing the most domain-relevant variations of the target.

3.3 Linear reduction with shift interventions

We further constrain the setting to be able to study the solution minimizing \mathcal{L}_{cons} analytically and get insights into how TCR works. In this section, we describe the approach for the 1D TCR, with $n = 1$ high-level cause. The case $n > 1$ is discussed in App. C.

Notation. We use boldface, *e.g.* \mathbf{i} , for column vectors, and \mathbf{i}_S for the subvector of \mathbf{i} restricted to the components in set S . When a vector, say $\boldsymbol{\tau}_k$, is associated to high-level SCM component k of a constructive transformation with alignment $\boldsymbol{\pi}$, $\bar{\boldsymbol{\tau}}_k$ indicates the restriction of $\boldsymbol{\tau}_k$ to components in $\boldsymbol{\pi}(k)$.

Tau map. To maximize interpretability, we assume a linear $\boldsymbol{\tau}$ -map, represented as a vector $\boldsymbol{\tau}$ such that:

$$\mathbf{X} \mapsto \begin{bmatrix} Y \\ Z \end{bmatrix} = \begin{bmatrix} \boldsymbol{\tau}_0^\top \\ \boldsymbol{\tau}_1^\top \end{bmatrix} \mathbf{X} = [\bar{\boldsymbol{\tau}}_0^\top \mathbf{X}_{\boldsymbol{\pi}(0)}, \bar{\boldsymbol{\tau}}_1^\top \mathbf{X}_{\boldsymbol{\pi}(1)}]^\top.$$

Omega map. We focus on *shift interventions* and map the vector \mathbf{i} of low-level interventions on the nodes in $\boldsymbol{\pi}(1)$ to a scalar shift intervention on the mechanism of Z_1 . We assume this map ω_1 to be linear and thus define the vector $\boldsymbol{\omega}_1$ such that the map is given by

$$\omega_1(\mathbf{i}) = \boldsymbol{\omega}_1^\top \mathbf{i} = \bar{\boldsymbol{\omega}}_1^\top \mathbf{i}_{\boldsymbol{\pi}(1)}.$$

Because it is a root node, intervening amounts to shifting the marginal distribution from $P^{(0)}(Z_1)$ to $P^{(\omega_1(\mathbf{i}))}(Z_1) = P^{(0)}(Z_1 - \omega_1(\mathbf{i}))$.

Choice of alignment $\boldsymbol{\pi}$. In order to form a constructive transformation we need to impose some restrictions on the alignment: (1) $\boldsymbol{\pi}(0)$ must include the support of $\boldsymbol{\tau}_0$, which is given; (2) $\boldsymbol{\pi}(1)$ must not overlap with $\boldsymbol{\pi}(0)$.

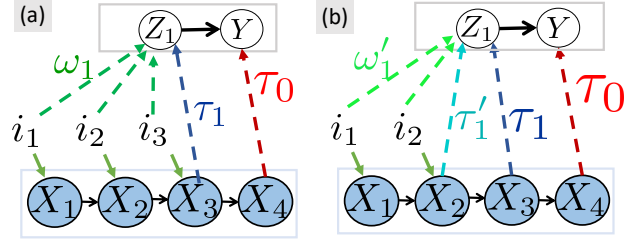


Figure 2: **TCR solutions on a chain graph.** Arrows indicate the non-zero coefficients of each map. (a) Unique solution $\boldsymbol{\tau}_1$ when interventions are on all nodes but the target. (b) Two solutions $\boldsymbol{\tau}_1$ and $\boldsymbol{\tau}'_1$ when interventions are on the first two nodes only.

Beyond that, there are potential degrees of freedom for $\boldsymbol{\pi}$, and users may want to incorporate domain knowledge as well as interpretability constraints to reduce the variables included in $\boldsymbol{\pi}(1)$. This can be done by fixing $\boldsymbol{\pi}$ prior to learning, or by adapting it during learning, using for example additional terms to the loss enforcing sparsity. Such sparsity enforcing regularizers are particularly useful for the case of $n \geq 2$ high-level causes, as shown in App. C. For the next identifiability results of Sec. 3.4, we will first fix $\boldsymbol{\pi}$ and show that different choices may lead to indeterminacies of the TCR solution.

Choice of prior $P(\mathbf{i})$. The solutions minimizing the loss of Eq. (4), may depend on the choice of the prior $P(\mathbf{i})$, and in particular on which variables are actually intervened on. For our theoretical analysis, we assume the prior has the following form.

Assumption 3.2. There exists a (unique) subset Ω of intervened low-level variables such that $P(\mathbf{i}_\Omega)$ has a density with respect to the Lebesgue measure, with support covering a neighborhood of zero (*i.e.* the unintervened case). Components of \mathbf{i} associated to unintervened variables (outside of Ω) take the deterministic value $\mathbf{i} = 0$.

3.4 Identifiability results

If we assume the low-level model is linear Gaussian of the form $\mathbf{X}_{\boldsymbol{\pi}(1)} \rightarrow \mathbf{X}_{\boldsymbol{\pi}(0)}$, we can show the existence and uniqueness of the solution, under the condition that $\boldsymbol{\pi}(1)$ contains all and only intervened variables.

Proposition 3.3. Assume the low-level SCM follows

$$\mathbf{X} := \mathbf{A}\mathbf{X} + \mathbf{U} + \mathbf{i}, \quad U_k \sim \mathcal{N}(\mu_k, \sigma_k^2), \quad \mathbf{i} \sim P(\mathbf{i})$$

such that \mathbf{X} and \mathbf{A} take the block forms

$$\mathbf{X} = \begin{bmatrix} \mathbf{X}_{\boldsymbol{\pi}(0)} \\ \mathbf{X}_{\boldsymbol{\pi}(1)} \end{bmatrix}, \quad \mathbf{A} = \begin{bmatrix} A_{00} & A_{01} \\ \mathbf{0} & A_{11} \end{bmatrix}.$$

Under Assum. 3.2, if $\Omega = \boldsymbol{\pi}(1)$, and for a given choice of target $Y = \boldsymbol{\tau}_0^\top \mathbf{X} = \bar{\boldsymbol{\tau}}_0^\top \mathbf{X}_{\boldsymbol{\pi}(0)}$, there is a unique linear

1D TCR, up to a multiplicative constant satisfying $\mathcal{L}_{cons} = 0$. It is given by

$$\bar{\tau}_1 = A_{01}^\top (I_{N_0} - A_{00})^{-\top} \bar{\tau}_0 \quad (7)$$

$$\text{and } \bar{\omega}_1 = (I_{N_1} - A_{11})^{-\top} \bar{\tau}_1. \quad (8)$$

Additionally, Assum. 3.2 can be replaced by Assum. B.2, which requires only a finite set of $\pi(1)$ interventions.

Interpretation. This solution is illustrated in Fig. 2(a) for a chain graph with $\pi(0) = \{4\}$ and $\pi(1) = \{1, 2, 3\}$. We can see that τ_1 puts all its weight on the unique parent of $X_4 = Y$. This can be seen as enforcing the mechanism consistency part of \mathcal{L}_{cons} . In contrast, ω_1 puts weight on all intervened variables, to enforce cause consistency of changes in Z_1 due to all interventions. In general, ω_1 and τ_1 will differ whenever there are causal interactions between variables in $\pi(1)$, encoded by A_{11} . See App. D for more details. This example shows that the set of intervened variables that affect shifts of Z_1 through ω_1 may strongly differ from those mapped by the reduction τ_1 . This may lead to conflicting interpretations of Z_1 , and will be addressed by regularization in Sec. 4.

Our next result shows that we lose identifiability of the TCR if we drop the assumption that all and only variables in $\pi(1)$ are intervened on.

Proposition 3.4. *Consider the setting of Prop. 3.3 with the exception that $\Omega \subsetneq \pi(1)$ such that there is now a non-empty subset $S = \pi(1) \setminus \Omega$, such that $\mathbf{X}_\Omega \rightarrow \mathbf{X}_S \rightarrow \mathbf{X}_{\pi(0)}$. Then there exist at least two different linear 1D TCR such that $\mathcal{L}_{cons} = 0$.*

This result can also be illustrated with a chain graph, as shown in Fig. 2(b). If the parent node X_3 of $Y = X_4$ is unintervened, then one may choose either $Z_1 = X_2$ or $Z_1 = X_3$ (matching the solution of Fig. 2(a)) to minimize \mathcal{L}_{cons} . This is because both variables are equivalently mediating all performed interventions to X_4 . Note that each choice has its own benefit: $Z_1 = X_3$, as a direct parent of Y , is a better statistical predictor of the value of Y . However, if we focus on causal interpretability of the high-level representation, $Z_1 = X_2$ is preferable because it is one of the variables intervened on at the low-level as enforced by the prior $P(\mathbf{i})$, and such that it will be associated to a non-zero weight in ω_1 for any solution satisfying $\mathcal{L}_{cons} = 0$.

This demonstrates that the choice of $\pi(1)$ may introduce ambiguities when searching for a consistent solution, and selecting where and how to intervene in the system plays a crucial role. While it is possible to restrict $\pi(1)$ to nodes that are directly intervened upon, some nodes may in practice be intervened on *sensu stricto*, while having a minimal impact on Y , yet they

may carry most of the weight of τ_1 . This again suggests a potential ‘‘inhomogeneity’’ between the high-level representation of the cause, with ω_1 and τ_1 reflecting different aspects of the low-level causes. To address this, we can enforce homogeneity of the solution by requiring ω and τ to be as similar as possible, which we implement as an optional regularization term of our learning objective in Sec. 4.

4 LINEAR TCR ALGORITHM

In this section, we introduce an algorithm to learn a linear reduction with shift interventions.

Gaussian approximation of consistency loss. Since the KL divergence is challenging to learn non-parametrically, we make a Gaussian assumption on the densities. This allows us to obtain an analytic expression for the loss based on second order statistics (see expression in App. E.1). In order to promote interpretability, we supplement \mathcal{L}_{cons} with a homogeneity regularizer.

Interventional homogeneity loss. Importantly, ω and τ can assign strong coefficients on different sets of variables. This is related to the causal structure of the set of variables constituting Z_k . This poses interpretability challenges, as the variables acted on are different from the variables used for prediction. To align those sets of variables, we introduce the *homogeneity loss* that is maximal when $\omega = \tau$, and scale invariant:

$$\mathcal{L}_{hom} = \sum_k \left\langle \frac{\omega_k}{\|\omega_k\|}, \frac{\tau_k}{\|\tau_k\|} \right\rangle. \quad (9)$$

Gathering the two losses, we get the total objective

$$\underset{\gamma, \tau_1, \omega_1}{\text{minimize}} \mathcal{L}_{tot} = \mathcal{L}_{cons} - \eta_h \mathcal{L}_{hom}.$$

The learning procedure is described in Algorithm 1.

5 EXPERIMENTS

5.1 Toy examples: linear Gaussian low-level causal models

Linear low-level causal models. We first test the proposed Algorithm 1 by sampling from a linear Gaussian low-level model, rather than a simulation. We construct linear models of the form shown in Proposition 3.3 by drawing the non-zero entries in the adjacency matrix uniformly from the interval $[-1, 1]$. We learn a targeted causal reduction with two high-level variables: the target Y and its single cause Z . Comprehensive experimental details can be found in App. F.

Algorithm 1 Linear TCR (LCPR)

Input λ : learning rate, $P(i)$: intervention prior, $Simulate(\theta, i, n_{sim})$: function returning n_{sim} paths, N_{ite} : number of iterations, B : simulation paths batch size, B_i : intervention batch size.

Output Estimated parameters $(\tau_1, \omega_1, \gamma)$.

Initialize τ_1, ω, γ

```

for  $m = 1..N_{ite}$  do
     $X, Y \leftarrow []$ 
    for  $l = 1..B_i$  do
         $i_l \leftarrow Sample(P(i))$ 
         $X_l = (x^1, \dots, x^B), Y_l \leftarrow Simulate(\theta, i_l, B)$ 
         $X \leftarrow [X[:, :], X_l]$ 
         $Y \leftarrow [Y[:, :], Y_l]$ 
         $I = [I[:, :], i_l]$ 
     $L_{tot} \leftarrow ComputeLoss(X, Y, I, \tau_1, \omega_1, \gamma)$ 
     $\nabla_\gamma, \nabla_\tau \leftarrow ComputeLossGradient(L_{tot})$ 
     $(\gamma, \tau_1, \omega_1) \leftarrow (\gamma - \lambda \nabla_\gamma, \tau_1 - \lambda \nabla_{\tau_1}, \omega_1 - \lambda \nabla_{\omega_1})$ 
    
```

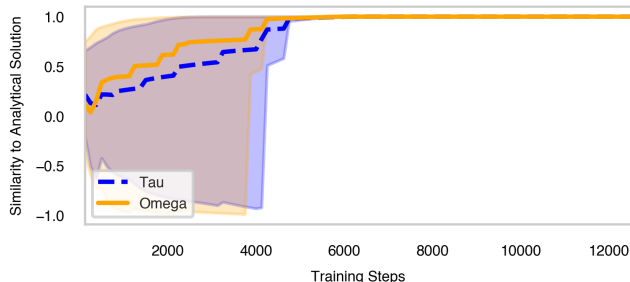


Figure 3: **Comparison between learned and analytical τ_1 and ω_1 parameters.** We show the average cosine similarity to the analytical solutions over 20 runs. Each run corresponds to one draw of adjacency matrix parameters. The shaded areas correspond to the range between the minimum and maximum values.

Fig. 3 compares the learned parameters τ_1 and ω_1 to the analytical solutions (7) and (8). We observe that, for these low-level models which meet the linear Gaussian assumption in Section 3, the learning algorithm converges to the global optimum.

Linear chain. To illustrate the behavior of TCR under homogeneity regularization (9), we consider a linear chain causal graph. In a chain graph, we constrain the adjacency matrix such that all nodes are connected along a chain of edges, with the target variable being the leaf node ($X_1 \rightarrow X_2 \rightarrow \dots \rightarrow Y$).

As depicted in Fig. 4, TCR attributes more significance to the low-level variables that are close ancestors in the causal graph (see interpretation in Sec. 3.3). By introducing homogeneity regularization (9), τ_1 and ω_1 become more congruent, enhancing interpretability. However, this regularization can reduce consistency (as elaborated in App. F).

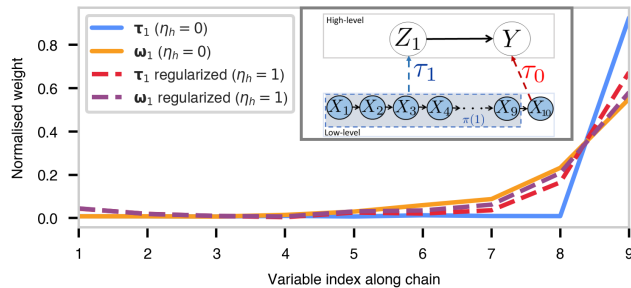


Figure 4: **Comparison of learned parameters τ_1 and ω_1 for chain graphs with and without homogeneity regularization.** The normalized τ_1 parameters $(\tau_1)_k / \sum_{k'} (\tau_1)_{k'}$, where k corresponds to the low-level variable index along the chain) are averaged over 20 runs. Each run corresponds to a draw of the adjacency parameters. Similarly, we depict the normalized ω_1 parameters. We compare two training settings: with and without homogeneity regularization (9) ($\eta_h = 0$ or $\eta_h = 1$, respectively). The inset shows the applied TCR scheme.

5.2 ODE simulation: Double Well

For a simulation based on an ODE system, we learn a targeted reduction of a ball moving in a double well potential under linear friction, as shown in Fig. 5. The state vector \mathbf{X} encodes the x -position and velocity in x -direction of the ball at each time steps of the simulation. As shift-interventions, we apply small random shifts of the ball’s velocity at each simulation time step, mimicking an applied external force. Initially, the ball starts on the left-hand side of the potential and starts oscillating. Since the ball experiences friction, it ends up in either the left or right minimum of the potential. The friction is relatively strong, such that, depending on the initial conditions and applied shift interventions, the ball either stays in the left well or crosses the middle hump once and stays in the right well (see Fig. 5(f)). We learn a simple targeted reduction with a single cause Z that explains the target Y . Further details about the ODE system and the learning parameters are given in App. F.

The learned τ_1 and ω_1 parameters are shown in Fig. 5(c) and (d). Note that due to the negative slope of the learned high-level causal mechanism (Fig. 5(e)), negative Z -values are mapped to predicting the right well as the final position, and vice versa. The τ_1 and ω_1 parameters for velocity are such that the larger the velocity is to the right, the lower Z and therefore the higher the predicted target Y . Similarly, for the position parameter: the more negative the position just before the critical point of the ball crossing the hump, the higher the probability of predicting to stay in the left well. This corresponds to the correct dynamics of the system and also identifies the main drivers that influence the outcome Y . Note that TCR does not

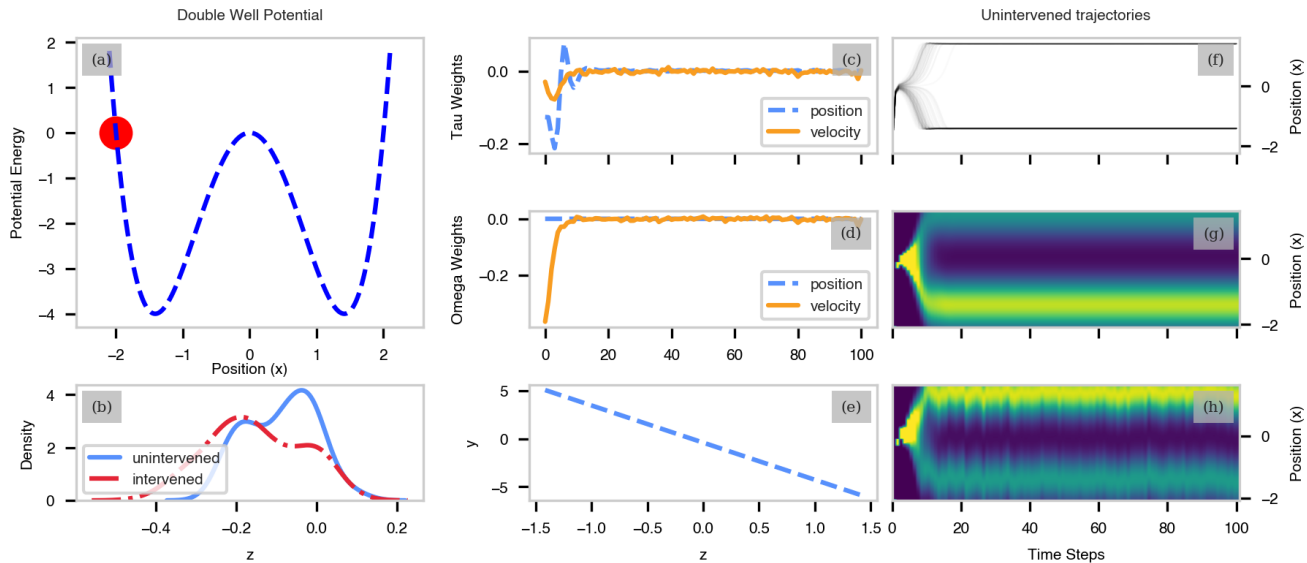


Figure 5: **Double well experiment.** Comparison of samples and inferred causal factors in the double well experiment. (a) Depicts the experimental setup with a ball moving in a double well potential subject to linear friction. (b) Displays the pushforward density of the high-level cause for the two settings: one where no intervention is applied (unintervened), and the other with an applied shift intervention. (c) and (d) represent the learned parameters, τ and ω , respectively. (e) Illustrates the conditional mean $\mathbb{E}[Y | Z]$ for the inferred high-level causal mechanism. (f) and (g) show samples from the unintervened setting and the corresponding estimated density. (h) Depicts the estimated density for the intervened setting.

focus on the part of \mathbf{X} which best predicts the final state of the system—like the position just before the end of the simulation. It rather highlights the variables which have the most impact on the target when they are intervened on, emphasizing the decisive time span when the ball either crosses the middle hump or stays in the left well.

6 RELATED WORK

Desiderata for CMR have been addressed theoretically by several works, in particular in the context of CFL (Chalupka et al., 2014, 2016), and subsequently with the notion of *exact transformations* (Rubenstein et al., 2017) and a more strongly constrained subclass: *causal abstractions* (Beckers and Halpern, 2019). An alternative framework for composing abstractions of finite models has been proposed by Rischel and Weichwald (2021). However, only few works have addressed how to build high-level representations from the low-level system data only. A line of works focuses on language models (Geiger and Straehle, 2020; Geiger et al., 2021, 2023a), where high-level variables and interpretations are readily available.

We start from the opposite direction and develop a general approach to build the high-level abstraction from the ground-up. Such a construction is done in CFL (Chalupka et al., 2014, 2016), where high-dimensional microscopic variables are turned into discrete high-level

variables. Zennaro et al. (2023) addressed this question in the context of finite and discrete domains, by minimizing the maximum Jensen-Shannon divergence over a finite set of perfect intervention distributions. In contrast with most works on CMR, our framework is fully compatible with imperfect (soft intervention) at the low level, which are more realistic and interpretable perturbations of many real-world systems than hard interventions. Soft interventions have been used for language model alignment (Geiger et al., 2023b), and their theoretical compatibility with the abstraction framework has been investigated by Massidda et al. (2023). Our approach aims at approximating an exact transformation, and is thus a relaxation of this setting.

Other theoretical frameworks for approximate abstractions have been proposed (Beckers et al., 2020; Rischel and Weichwald, 2021). Our work differs by providing an explicit loss well-suited to continuous causal models, that can be optimized efficiently and provide interpretable outcomes thanks to a cause-mechanism decomposition, a lower bound, and analytic solutions.

The way we relax constraints on low-level interventions shares also similarities with the views of Zhu et al. (2023) who consider stochastic low-level do-interventions sampled according to the observational distribution, our work is instead focused on soft-interventions, for which we impose a prior distribution, reflecting the relative importance that we put on them.

Our optimization objective is averaged over this prior, such that it plays a role in the final solution.

Our approach also relates to the search for optimal interventional or counterfactual manipulations to steer the output of a system to a particular value or distribution (Amos et al., 2018; Besserve et al., 2020) or to best explain an observation (Budhathoki et al., 2022; Von Kügelgen et al., 2023). We are in a way also selecting particular manipulations, but through the choice of dimensionality reduction ω , such that they are interpretable at a high level.

Finally, our approach relates to several works in causal representation learning, which have addressed identifiability of latent causal models from observational data, with (Liang et al., 2023) or without (Squires et al., 2023; von Kügelgen et al., 2023) assumptions on the latent causal graph. In contrast to those works, TCR does not assume an injective mapping of the mapping of the observations to the latent variables, such that the high-level model typically loses information relative to the low-level model.

7 DISCUSSION

Summary. We introduce a novel approach for understanding complex simulations by learning high-level causal explanations from low-level models. We propose the Targeted Causal Reduction (TCR) framework, which leverages interventions in the low-level model to obtain simplified, high-level representations of the causes of a target phenomenon. We formulate the intervention-based consistency constraint as an information theoretic learning objective, and provide theoretical interpretations and justifications for it. By further enforcing linearity and Gaussianity assumptions, and using shift interventions, we provide analytical solutions and study their uniqueness. This provides insights into TCR’s governing principles and potential weaknesses, which we address through regularization. We provide an algorithm for linear TCR and show it can effectively uncover the key causal factors influencing a phenomenon of interest. We demonstrate the algorithm’s capabilities through applications to both synthetic and scientific models, highlighting its potential for addressing the challenges posed by increasingly complex systems in scientific research.

Limitations and future work. To foster interpretability and tractability, we made Gaussian approximations and used linear τ and ω maps. While this has computational and interpretability benefits, this may be too limiting for some complex simulations, and future work should explore more flexible approaches. Additionally, our method relies on performing a large

number of interventions in simulation runs, which represents an additional cost in the context of large-scale simulation. How to make the algorithm scale to this setting is left to future work.

References

- B. Amos, I. D. J. Rodriguez, J. Sacks, B. Boots, and J. Z. Kolter. Differentiable MPC for end-to-end planning and control. *arXiv preprint arXiv:1810.13400*, 2018. [Cited on page 9.]
- S. Beckers and J. Y. Halpern. Abstracting causal models. In *Proceedings of the aaai conference on artificial intelligence*, volume 33, pages 2678–2685, 2019. [Cited on pages 2, 3, and 8.]
- S. Beckers, F. Eberhardt, and J. Y. Halpern. Approximate causal abstractions. In *Uncertainty in artificial intelligence*, pages 606–615. PMLR, 2020. [Cited on pages 2 and 8.]
- M. Besserve and B. Schölkopf. Learning soft interventions in complex equilibrium systems. In *Uncertainty in Artificial Intelligence*, pages 170–180. PMLR, 2022. [Cited on page 2.]
- M. Besserve, A. Mehrjou, R. Sun, and B. Schölkopf. Counterfactuals uncover the modular structure of deep generative models. In *ICLR2020*, 2020. [Cited on page 9.]
- B. Biswas, S. Chatterjee, S. Mukherjee, and S. Pal. A discussion on euler method: A review. *Electronic Journal of Mathematical Analysis and Applications*, 1(2):2090–2792, 2013. [Cited on page 11.]
- S. Bongers, P. Forré, J. Peters, and J. M. Mooij. Foundations of structural causal models with cycles and latent variables. *The Annals of Statistics*, 49(5):2885–2915, 2021. [Cited on page 12.]
- M. Breakspear. Dynamic models of large-scale brain activity. *Nature neuroscience*, 20(3):340–352, 2017. [Cited on page 1.]
- K. Budhathoki, L. Minorics, P. Blöbaum, and D. Janzing. Causal structure-based root cause analysis of outliers. In *International Conference on Machine Learning*, pages 2357–2369. PMLR, 2022. [Cited on page 9.]
- K. Chalupka, P. Perona, and F. Eberhardt. Visual causal feature learning. *arXiv preprint arXiv:1412.2309*, 2014. [Cited on pages 3 and 8.]
- K. Chalupka, T. Bischoff, P. Perona, and F. Eberhardt. Unsupervised discovery of el nino using causal feature learning on microlevel climate data. *arXiv preprint arXiv:1605.09370*, 2016. [Cited on pages 3 and 8.]
- G. Deco and M. L. Kringelbach. Great expectations: using whole-brain computational connectomics for understanding neuropsychiatric disorders. *Neuron*, 84(5):892–905, 2014. [Cited on page 1.]
- A. Geiger, H. Lu, T. Icard, and C. Potts. Causal abstractions of neural networks. *Advances in Neural Information Processing Systems*, 34:9574–9586, 2021. [Cited on page 8.]
- A. Geiger, C. Potts, and T. Icard. Causal abstraction for faithful model interpretation. *arXiv preprint arXiv:2301.04709*, 2023a. [Cited on pages 3 and 8.]

- A. Geiger, Z. Wu, C. Potts, T. Icard, and N. D. Goodman. Finding alignments between interpretable causal variables and distributed neural representations. *arXiv preprint arXiv:2303.02536*, 2023b. [Cited on page 8.]
- P. Geiger and C.-N. Straehle. Learning game-theoretic models of multiagent trajectories using implicit layers. *arXiv preprint arXiv:2008.07303*, 2020. [Cited on page 8.]
- H. Grassl. Status and improvements of coupled general circulation models. *Science*, 288(5473):1991–1997, 2000. [Cited on page 1.]
- R. Jenatton, J.-Y. Audibert, and F. Bach. Structured variable selection with sparsity-inducing norms. *The Journal of Machine Learning Research*, 12:2777–2824, 2011. [Cited on pages 18 and 19.]
- W. Liang, A. Kekić, J. von Kügelgen, S. Buchholz, M. Besserve, L. Gresele, and B. Schölkopf. Causal component analysis. *arXiv preprint arXiv:2305.17225*, 2023. [Cited on page 9.]
- R. Massidda, A. Geiger, T. Icard, and D. Bacciu. Causal abstraction with soft interventions. In *2nd Conference on Causal Learning and Reasoning*, 2023. [Cited on page 8.]
- A. Millet and P.-L. Morien. On implicit and explicit discretization schemes for parabolic spdes in any dimension. *Stochastic Processes and their Applications*, 115(7):1073–1106, 2005. [Cited on page 12.]
- J. Pearl. *Causality*. Cambridge university press, second edition, 2009. [Cited on page 1.]
- J. Peters, D. Janzing, and B. Schölkopf. *Elements of Causal Inference – Foundations and Learning Algorithms*. MIT Press, 2017. [Cited on page 2.]
- M. Reichstein, G. Camps-Valls, B. Stevens, M. Jung, J. Denzler, N. Carvalhais, and f. Prabhat. Deep learning and process understanding for data-driven earth system science. *Nature*, 566(7743):195–204, 2019. [Cited on page 1.]
- E. F. Rischel and S. Weichwald. Compositional abstraction error and a category of causal models. In *Uncertainty in Artificial Intelligence*, pages 1013–1023. PMLR, 2021. [Cited on page 8.]
- P. K. Rubenstein, S. Weichwald, S. Bongers, J. M. Mooij, D. Janzing, M. Grosse-Wentrup, and B. Schölkopf. Causal consistency of structural equation models. *arXiv preprint arXiv:1707.00819*, 2017. [Cited on pages 2, 3, and 8.]
- S. Safavi, T. I. Panagiotaropoulos, V. Kapoor, J. F. Ramirez-Villegas, N. K. Logothetis, and M. Besserve. Uncovering the organization of neural circuits with generalized phase locking analysis. *PLOS Computational Biology*, 19(4):e1010983, 2023. [Cited on page 1.]
- T. Sauer. Computational solution of stochastic differential equations. *Wiley Interdisciplinary Reviews: Computational Statistics*, 5(5):362–371, 2013. [Cited on pages 3 and 11.]
- C. Squires, A. Seigal, S. Bhate, and C. Uhler. Linear causal disentanglement via interventions. In *40th International Conference on Machine Learning*, 2023. [Cited on page 9.]
- J. von Kügelgen, M. Besserve, W. Liang, L. Gresele, A. Kekić, E. Bareinboim, D. M. Blei, and B. Schölkopf. Nonparametric identifiability of causal representations from unknown interventions. *arXiv preprint arXiv:2306.00542*, 2023. [Cited on page 9.]
- J. Von Kügelgen, A. Mohamed, and S. Beckers. Backtracking counterfactuals. In *Conference on Causal Learning and Reasoning*, pages 177–196. PMLR, 2023. [Cited on page 9.]
- F. M. Zennaro, M. Drávucz, G. Apachitei, W. D. Widanage, and T. Damoulas. Jointly learning consistent causal abstractions over multiple interventional distributions. *arXiv preprint arXiv:2301.05893*, 2023. [Cited on page 8.]
- Y. Zhu, K. Budhathoki, J. Kuebler, and D. Janzing. Meaningful causal aggregation and paradoxical confounding. *arXiv preprint arXiv:2304.11625*, 2023. [Cited on page 8.]

Supplementary Materials

A SUPPLEMENTAL BACKGROUND

A.1 Numerical schemes for simulations

Methods for the numerical approximations of scientific models is a broad area spanning multiple fields. We provide here a few elements based on a 1D example to justify how these models relate to SCMs. The Euler method (Biswas et al., 2013), can be used to approximate a 1D ODE of the form

$$\begin{cases} x(t_0) = x_0, \\ \frac{dx}{dt} = F(x(t)), \end{cases}$$

with F smooth real-valued function, using a discretized time grid with time step Δt . The finite difference approximation of the derivative

$$x(t + \Delta t) - x(t) \approx \Delta t \cdot \frac{dx}{dt},$$

leads to the iterative numerical scheme for the approximation $\hat{x}(k\Delta t)$:

$$\begin{cases} \hat{x}(t_0) = x_0, \\ \hat{x}(t_0 + (k+1)\Delta t) = \hat{x}(t_0 + k\Delta t) + \Delta t \cdot F(\hat{x}(t_0 + k\Delta t)), \quad k > 0. \end{cases}$$

This scheme is called *explicit* because future values depend explicitly on past ones. In that case, one may define the N low-level endogenous variables as $\mathbf{X} = [\hat{x}(t_0 + \Delta t), \dots, \hat{x}(t_0 + N\Delta t)]^\top$. They can be seen as pertaining to a chain SCM with structural equations

$$\begin{cases} \widehat{X}_1 := x_0 + \Delta t \cdot F(x_0) \\ \widehat{X}_{k+1} := \widehat{X}_k + \Delta t \cdot F(\widehat{X}_k), \quad k > 1. \end{cases}$$

Because the ODE describes deterministic dynamics, the corresponding SCM is deterministic as well, i.e. exogenous variables can be taken as trivial zero constants. However, if we turn this ODE into the following 1D SDE

$$\begin{cases} X(t_0) = x_0, \\ dX = F(X(t))dt + \sigma_W \cdot dW, \end{cases}$$

where W is a standard Brownian motion, then the Euler-Murayama method generalizes the previous approximation (Sauer, 2013), and leads to an updated SCM with structural equation

$$\begin{cases} \widehat{X}_1 := x_0 + \Delta t \cdot F(x_0) + U_1 \\ \widehat{X}_{k+1} := \widehat{X}_k + \Delta t \cdot F(\widehat{X}_k) + U_{k+1}, \quad k > 1, \end{cases}$$

where the exogenous variables U_k represent the increments of the scaled Brownian motion $\sigma_W \cdot W$ between successive time steps, and are thus jointly independent Gaussian due to fundamental properties of Brownian motion.

This approach generalizes to explicit numerical schemes for multivariate ODE and SDEs where the state variable \mathbf{X} lives in \mathbb{R}^n . As an illustration we can take the following class of SDE models

$$\begin{cases} \mathbf{X}(t_0) = \mathbf{x}_0, \\ d\mathbf{X} = \mathbf{F}(\mathbf{X}(t))dt + \boldsymbol{\sigma}_W \cdot d\mathbf{W}, \end{cases}$$

with $\mathbf{F} : \mathbb{R}^n \rightarrow \mathbb{R}^n$, $\boldsymbol{\sigma}_W = \mathbb{R}^{(n \times n)}$, and \mathbf{W} a n -dimensional standard Brownian motion. This leads to the scheme

$$\begin{cases} \widehat{\mathbf{X}}_1 := \mathbf{x}_0 + \Delta t \cdot \mathbf{F}(\mathbf{x}_0) + \mathbf{U}_1 \\ \widehat{\mathbf{X}}_{k+1} := \widehat{\mathbf{X}}_k + \Delta t \cdot \mathbf{F}(\widehat{\mathbf{X}}_k) + \mathbf{U}_{k+1}, \quad k > 1, \end{cases}$$

where the \mathbf{U}_k are now multivariate Gaussian variables, whose components may or may not be independent depending on the choice of the matrix σ_W . If the exogenous components are independent, the variables can be described by a standard SCM as introduced in main text. If the exogenous components are dependent, the variables can be described by a more general notion of SCM, allowing hidden confounding (Bongers et al., 2021).

Further generalization to numerical schemes for Stochastic Partial Differential Equations (SPDEs) using finite difference approximations for partial derivatives with respect to other variables than time are also possible (Millet and Morien, 2005).

A.2 Reduction of the Euler scheme for a system of point masses

In the context of the main text example, we assume each point Mass is submitted to a fluid friction force opposing its movement with fixed coefficient λ . Masses are moreover intervened on via additional external forces $\{\mathbf{f}_k\}$. Finally, internal forces are exerted on mass k by other point masses of the system, summing up to \mathbf{g}_k . Newton's second law applied to individual masses results in the following system of 2D vector equations

$$m_k \frac{d\mathbf{v}_k}{dt} = -\lambda \mathbf{v}_k(t) + \mathbf{f}_k(t) + \mathbf{g}_k(t).$$

We can approximate each equation to estimate iteratively the x and y components of the speed of individual point masses in the system, using a small time-step Δt , such that we get the discrete time estimates $\hat{v}_{x,k}[n] \approx v_{x,k}(n\Delta t)$ and $\hat{v}_{y,k}[n] \approx v_{y,k}(n\Delta t)$ satisfying

$$\begin{aligned} m_k \cdot \hat{v}_{x,k}[n+1] &:= (1 - \Delta t \lambda) \cdot m_k \cdot \hat{v}_{x,k}[n] + \Delta t \cdot f_{x,k}(n\Delta t) + \Delta t \cdot g_{x,k}(n\Delta t), \\ m_k \cdot \hat{v}_{y,k}[n+1] &:= (1 - \Delta t \lambda) \cdot m_k \cdot \hat{v}_{y,k}[n] + \Delta t \cdot f_{y,k}(n\Delta t) + \Delta t \cdot g_{y,k}(n\Delta t). \end{aligned}$$

Here, f represents external forces, λ is a viscous damping coefficient, and g denotes internal forces. We consider \mathbf{i} to be the vector of all components of external forces, and the target variable to be the final horizontal speed of the center of mass at iteration N . From the physics of freely moving systems of points, it is clear that the target variable can be predicted by considering only the horizontal dynamics of the center of mass. More precisely, we integrate the sum of external forces over the time span of the experiment, and use the last intervened time point n_f to predict the final outcome of the simulation, leading to the reduction

$$\begin{aligned} Z_1^{(\omega(\mathbf{i}))} &= \left(\sum_k m_k \right) v_{x,G}[n_f] = \sum_k m_k v_{x,k}[n_f] = \Delta t \sum_{n=0}^{n_f} (1 - \Delta t \lambda)^{(n_f-n)} \sum_k f_{x,k}(n\Delta t), \\ Y = v_{x,G}[N] &:= (1 - \Delta t \lambda)^{(N-n_f)} Z_1 + \sum_{n=n_f+1}^N \sum_k f_{x,k}(n\Delta t). \end{aligned}$$

To make the notation compatible with those use used in our TCR framework, we can gather all speed variables in a high-dimensional vector \mathbf{X} and all external force variables in a vector \mathbf{i} , the high-level causal model is thus generated by a linear τ -map and linear ω map for shift interventions, taking the form of the exact transformation

$$Z_1 = \tau_1^\top \mathbf{X} + \omega_1^\top \mathbf{i}, \quad Y = \tau_0^\top \mathbf{X} + \omega_0^\top \mathbf{i} := f(Z_1).$$

where the term $\omega_0^\top \mathbf{i}$ accounts for interventions happening between discrete times $n_f + 1$ and N and thus affect Y without being mediated by Z_1 . In our framework, only interventions mediated by the cause, reflected in the term $\omega_1^\top \mathbf{i}$, are accounted for in the high-level model.

A.3 Constructive transformations

We complete the main text definition to include the constraint on the intervention map ω

Definition A.1. $(\tau, \omega) : (\mathcal{X} \rightarrow \mathcal{Z}, \mathcal{I} \rightarrow \mathcal{J})$ is a constructive $(\tau - \omega)$ -transformation between model \mathcal{L} and \mathcal{H} if there exists an alignment map π mapping each high-level endogenous variable to a subset of low-level endogenous variables such that for all $k \neq l$, $\pi(k) \cap \pi(l) = \emptyset$ and we have both

- for each component τ_k of τ there exists a function $\bar{\tau}_k$ such that for all \mathbf{x} in \mathcal{X} ,

$$\tau_k(\mathbf{x}) = \bar{\tau}_k(\mathbf{x}_{\pi(k)});$$

- for each component ω_k of ω there exists a function $\bar{\omega}_k$ such that for all \mathbf{i} in \mathcal{I} ,

$$\omega_k(\mathbf{i}) = \bar{\omega}_k(\mathbf{i}_{\pi(k)}).$$

B PROOF OF MAIN TEXT RESULTS

B.1 Proof of Proposition 3.1

We first reformulate Proposition 3.1 more formally as follows.

Proposition B.1. *The consistency loss is positive, invariant to invertible reparametrizations as defined in Definition D.1, and vanishes if and only if the transformation is exact for almost all interventions. It admits the following decomposition:*

$$\mathcal{L}_{cons} = \mathbb{E}_{\mathbf{i} \sim P(\mathbf{i})} \left[KL \left(\widehat{P}_{\tau}^{(\mathbf{i})}(\mathbf{Z}) \parallel P^{(\omega(\mathbf{i}))}(\mathbf{Z}) \right) + \mathbb{E}_{\mathbf{z} \sim \widehat{P}_{\tau}^{(\mathbf{i})}(\mathbf{Z})} \left[KL \left(\widehat{P}_{\tau}^{(\mathbf{i})}(Y|\mathbf{z}) \parallel P^{(0)}(Y|\mathbf{z}) \right) \right] \right], \quad (10)$$

and is an upper bound of the causal relevance loss

$$\mathcal{L}_{rel} = \mathbb{E}_{\mathbf{i} \sim P(\mathbf{i})} \left[KL \left(\widehat{P}^{(\mathbf{i})}(Y) \parallel P^{(\omega(\mathbf{i}))}(Y) \right) \right] \leq \mathcal{L}_{cons}. \quad (11)$$

Proof. **Positivity** of the loss comes from the positivity of the KL-divergence. Taking the expectation of this divergence with respect to $P(\mathbf{i})$ thus must be positive too.

Invariance to reparameterizations.

We assume a reparametrization ρ designed according to the framework introduced in Appendix D.1. By invariance of the KL divergence to invertible transformations, we have equality between the KL associated to the two different reductions (τ, ω) and $(\rho \circ \tau, \psi \circ \omega)$:

$$KL \left(\widehat{P}_{\tau}^{(\mathbf{i})}(Y, \mathbf{Z}) \parallel P_{\mathcal{H}, \gamma}^{(\omega(\mathbf{i}))}(Y, \mathbf{Z}) \right) = KL \left(\tilde{\rho}_{\#} [\widehat{P}_{\tau}^{(\mathbf{i})}(Y, \mathbf{Z})] \parallel \tilde{\rho}_{\#} [P_{\mathcal{H}, \gamma}^{(\omega(\mathbf{i}))}(Y, \mathbf{Z})] \right) = KL \left(\widehat{P}_{\rho \circ \tau}^{(\mathbf{i})}(Y, \mathbf{Z}) \parallel P_{\mathcal{H}, \gamma'}^{(\psi \circ \omega(\mathbf{i}))}(Y, \mathbf{Z}) \right).$$

The transformation (ρ, ψ) thus leaves \mathcal{L}_{cons} invariant.

Cause-mechanism decomposition. Under our setting (see Sec. 3.1), the interventional distribution of the high-level causal model factorizes as

$$P^{(\omega(\mathbf{i}))}(Y, \mathbf{Z}) = P^{(0)}(Y|\mathbf{Z}) P^{(\omega(\mathbf{i}))}(\mathbf{Z}).$$

The pushforward (by reduction) of the interventional distribution of the low-level model factorizes as

$$\widehat{P}^{(\mathbf{i})}(Y, \mathbf{Z}) = \widehat{P}^{(\mathbf{i})}(Y|\mathbf{Z}) \widehat{P}^{(\mathbf{i})}(\mathbf{Z}),$$

$$\text{with } \widehat{P}^{(\mathbf{i})}(\mathbf{Z}) = \tau_{1, \#} [P^{(\mathbf{i})}(X_{\pi(1)})] \text{ and } \widehat{P}^{(\mathbf{i})}(Y|\mathbf{Z}) = \frac{\tau_{\#} [P^{(\mathbf{i})}(X_{\pi(0)}, X_{\pi(1)})]}{\tau_{1, \#} [P^{(\mathbf{i})}(X_{\pi(1)})]}.$$

Thus, the KL divergence can be decomposed as

$$\begin{aligned} & KL \left(\widehat{P}^{(\mathbf{i})}(Y, \mathbf{Z}) \parallel P^{(\omega(\mathbf{i}))}(Y, \mathbf{Z}) \right) \\ &= \int_{\mathbf{y}} \int_{\mathbf{z}} \widehat{P}^{(\mathbf{i})}(Y, \mathbf{Z}) \log \frac{\widehat{P}^{(\mathbf{i})}(Y, \mathbf{Z})}{P^{(\omega(\mathbf{i}))}(Y, \mathbf{Z})} d\mathbf{Z} dY \\ &= \int_{\mathbf{y}} \int_{\mathbf{z}} \widehat{P}^{(\mathbf{i})}(Y|\mathbf{Z}) \widehat{P}^{(\mathbf{i})}(\mathbf{Z}) \log \frac{\widehat{P}^{(\mathbf{i})}(Y|\mathbf{Z}) \widehat{P}^{(\mathbf{i})}(\mathbf{Z})}{P^{(0)}(Y|\mathbf{Z}) P^{(\omega(\mathbf{i}))}(\mathbf{Z})} d\mathbf{Z} dY \\ &= KL_Z \left(\widehat{P}^{(\mathbf{i})}(\mathbf{Z}) \parallel P^{(\omega(\mathbf{i}))}(\mathbf{Z}) \right) + \mathbb{E}_{\mathbf{z} \sim \widehat{P}^{(\mathbf{i})}(\mathbf{Z})} \left[KL_Y \left(\widehat{P}^{(\mathbf{i})}(Y|\mathbf{Z} = \mathbf{z}) \parallel P^{(0)}(Y|\mathbf{Z} = \mathbf{z}) \right) \right] \\ &= KL_Z \left(\widehat{P}^{(\mathbf{i})}(\mathbf{Z}) \parallel P^{(\omega(\mathbf{i}))}(\mathbf{Z}) \right) + KL_{Y, \mathbf{Z}} \left(\widehat{P}^{(\mathbf{i})}(\widehat{Y}, \mathbf{Z}) \parallel P^{(0)}(Y|\mathbf{Z}) \widehat{P}^{(\mathbf{i})}(\mathbf{Z}) \right). \end{aligned}$$

The first term is a cause consistency loss (same principle but for that variable only). The second term can be thought of as a mechanism consistency, where we use the ground truth low-level cause distribution to probe the similarity of the outputs of the “true” (in fact, the conditional distribution) and approximate mechanism. Our interpretability choice prevents the high-level mechanism to be intervened on, so a single stochastic map (i.e. a Markov kernel) must fit at best all the sampled experimental conditionals.

Lower bounding by causal relevance We may ask the question of causal relevance of high-level causes. One way to quantify this is to assess whether the variations of the target due to low-level interventions are well captured by high-level interventions, which can be measured by a KL divergence on the target’s marginal

$$\mathcal{L}_{rel} = \mathbb{E}_{\mathbf{i} \sim p(\mathbf{i})} \left[KL_Y \left(\widehat{P}^{(\mathbf{i})}(Y) \parallel P^{(\omega(\mathbf{i}))}(Y) \right) \right].$$

Note: In the Gaussian 1D case, this gives

$$\frac{1}{2} \mathbb{E}_{\mathbf{i} \sim p(\mathbf{i})} \left[\frac{(\mu_Y + \alpha \omega^\top \mathbf{i} - \widehat{\mu}_Y^{(\mathbf{i})})^2}{\sigma_Y^2} + \frac{\widehat{\sigma}_Y^{2(\mathbf{i})}}{\sigma_Y^2} - \ln \left(\frac{\widehat{\sigma}_Y^{2(\mathbf{i})}}{\sigma_Y^2} \right) - 1 \right].$$

Interestingly, we can break down this term using

$$\begin{aligned} & KL \left(\widehat{P}^{(\mathbf{i})}(Y, \mathbf{Z}) \parallel P^{(\omega(\mathbf{i}))}(Y, \mathbf{Z}) \right) \\ &= KL_Y \left(\widehat{P}^{(\mathbf{i})}(Y) \parallel P^{(\omega(\mathbf{i}))}(Y) \right) + \mathbb{E}_{y \sim \widehat{P}^{(\mathbf{i})}(Y)} \left[KL_Y \left(\widehat{P}^{(\mathbf{i})}(\mathbf{Z}|Y=y) \parallel P^{(\omega(\mathbf{i}))}(\mathbf{Z}|Y=y) \right) \right] \end{aligned}$$

where both terms are positive by positivity of the KL divergence. As a consequence,

$$\begin{aligned} KL_Y \left(\widehat{P}^{(\mathbf{i})}(Y) \parallel P^{(\omega(\mathbf{i}))}(Y) \right) &= KL \left(\widehat{P}^{(\mathbf{i})}(Y, \mathbf{Z}) \parallel P^{(\omega(\mathbf{i}))}(Y, \mathbf{Z}) \right) - \mathbb{E}_{y \sim \widehat{P}^{(\mathbf{i})}(Y)} \left[KL_Y \left(\widehat{P}^{(\mathbf{i})}(\mathbf{Z}|Y=y) \parallel P^{(\omega(\mathbf{i}))}(\mathbf{Z}|Y=y) \right) \right] \\ &\leq KL \left(\widehat{P}^{(\mathbf{i})}(\widehat{Y}, \mathbf{Z}) \parallel P^{(\omega(\mathbf{i}))}(Y, \mathbf{Z}) \right) = \mathcal{L}_{cons}. \end{aligned}$$

so the minimized consistency loss is an upper bound to causal relevance. \square

B.2 Proof of Proposition 3.3

Proposition 3.3. *Assume the low-level SCM follows*

$$\mathbf{X} := A\mathbf{X} + \mathbf{U} + \mathbf{i}, \quad U_k \sim \mathcal{N}(\mu_k, \sigma_k^2), \quad \mathbf{i} \sim P(\mathbf{i})$$

such that \mathbf{X} and A take the block forms

$$\mathbf{X} = \begin{bmatrix} \mathbf{X}_{\pi(0)} \\ \mathbf{X}_{\pi(1)} \end{bmatrix}, \quad A = \begin{bmatrix} A_{00} & A_{01} \\ \mathbf{0} & A_{11} \end{bmatrix}.$$

Under Assum. 3.2, if $\Omega = \pi(1)$, and for a given choice of target $Y = \tau_0^\top \mathbf{X} = \bar{\tau}_0^\top \mathbf{X}_{\pi(0)}$, there is a unique linear 1D TCR, up to a multiplicative constant satisfying $\mathcal{L}_{cons} = 0$. It is given by

$$\bar{\tau}_1 = A_{01}^\top (I_{N_0} - A_{00})^{-\top} \bar{\tau}_0 \tag{7}$$

$$\text{and } \bar{\omega}_1 = (I_{N_1} - A_{11})^{-\top} \bar{\tau}_1. \tag{8}$$

In addition to the proof of this proposition, we are going to show that Assum. 3.2 can be replaced by the following Assum. B.2 in this proposition, to yield the same result.

Assumption B.2. $P(\mathbf{i}_{\pi(1)})$ is a mixture of $\pi(1) + 1$ distinct diracs, including one at zero. The remaining components have constant value zero.

Proof. We exploit the positive definiteness of the KL loss and its continuity with respect to \mathbf{i} . Since the variables are jointly Gaussian, continuity is obvious from the analytical expression of the KL for Gaussian variables and continuity of the shift operation applied to the parameters of the Gaussian. We exploit the cause-mechanism decomposition and the lower-bound by \mathcal{L}_{cons} to progressively identify necessary conditions on parameters to have $\mathcal{L}_{cons} = 0$ and finally check those conditions are sufficient.

Let N_0 be the size of $\pi(0)$ and N_1 be the size of $\pi(1)$. Because of the SCM assumption, the causal graph is a DAG, such that variables can be ordered without loss of generality such that A (and thus A_{00} and A_{11}) is strictly upper triangular. This entails that $(I_N - A)$ is invertible (as an upper triangular matrix with non-zero diagonal coefficients). The low-level variables then satisfy

$$\mathbf{X}^{(i)} = (I_N - A)^{-1}(\mathbf{U} + \mathbf{i})$$

where

$$(I_N - A)^{-1} = \begin{bmatrix} (I_{N_0} - A_{00})^{-1}, & (I_{N_0} - A_{00})^{-1}A_{01}(I_{N_1} - A_{11})^{-1} \\ 0 & (I_{N_1} - A_{11})^{-1} \end{bmatrix}$$

leading to the pushforward high-level cause variable

$$\widehat{\mathbf{Z}}_1^{(i)} = \bar{\boldsymbol{\tau}}_1^\top (I_N - A)^{-1}(\mathbf{U} + \mathbf{i}) = \bar{\boldsymbol{\tau}}_1^\top (I_{N_1} - A_{11})^{-1}(\mathbf{U}_{\pi(1)} + \mathbf{i}_{\pi(1)}).$$

Looking for the solutions satisfying $\mathcal{L}_{cons} = 0$ entails that they must satisfy that for almost all \mathbf{i} , this push-forward distribution matches the learned high-level interventional distribution which satisfies

$$P^{(\omega_1(\mathbf{i}))}(Z_1) = P^{(0)}(Z_1 - \omega_1^\top(\mathbf{i})).$$

According to Assum. 3.2, and since we assume $\Omega = \pi(1)$, the prior $P(\mathbf{i}_{\pi(1)})$ has density with respect to the Lebesgue measure with support including a neighborhood of $\mathbf{i} = \mathbf{0}$, by continuity of the KL divergence, a solution making the consistency loss vanish needs to have the KL divergence term vanish for $\mathbf{i} = \mathbf{0}$ (otherwise we could find a neighborhood of $\mathbf{i} = \mathbf{0}$ such that the KL does not vanish, by continuity of the KL divergence).

This vanishing of the KL divergence entails that its terms: the two unintervened densities, are equal, such that we get

$$P^{(0)}(Z_1) = (\bar{\boldsymbol{\tau}}_1^\top (I_{N_1} - A_{11})^{-1})_{\#} P(\mathbf{U}) = \mathcal{N}(\bar{\boldsymbol{\tau}}_1^\top (I_N - A_{11})^{-1} \boldsymbol{\mu}_{\mathbf{U}_1}, \bar{\boldsymbol{\tau}}_1^\top (I_N - A_{11})^{-1} \boldsymbol{\Sigma}_{\mathbf{U}_{\pi(1)}} (I_N - A_{11})^{-\top} \bar{\boldsymbol{\tau}}_1),$$

which entails

$$\sigma_{Z,1}^2 = \bar{\boldsymbol{\tau}}_1^\top (I_N - A_{11})^{-1} \boldsymbol{\Sigma}_{\mathbf{U}_{\pi(1)}} (I_N - A_{11})^{-\top} \bar{\boldsymbol{\tau}}_1 \quad (12)$$

and

$$\boldsymbol{\mu}_{Z,1} = \bar{\boldsymbol{\tau}}_1^\top (I_N - A_{11})^{-1} \boldsymbol{\mu}_{\mathbf{U}_{\pi(1)}}. \quad (13)$$

For the same reasons, we can further match the interventional distributions in an open set included in the interior of the support of $P(\mathbf{i})$, such that for all \mathbf{i} in this open set

$$\begin{aligned} \mathcal{N}(\bar{\boldsymbol{\tau}}_1^\top (I_{N_1} - A_{11})^{-1}(\boldsymbol{\mu}_{\mathbf{U}_1} + \mathbf{i}), \bar{\boldsymbol{\tau}}_1^\top (I_{N_1} - A_{11})^{-1} \boldsymbol{\Sigma}_{\mathbf{U}_1} (I_{N_1} - A_{11})^{-\top} \bar{\boldsymbol{\tau}}_1) \\ = \mathcal{N}(\bar{\boldsymbol{\tau}}_1^\top (I_{N_1} - A_{11})^{-1} \boldsymbol{\mu}_{\mathbf{U}_1} + \boldsymbol{\omega}_1^\top \mathbf{i}, \bar{\boldsymbol{\tau}}_1^\top (I_{N_1} - A_{11})^{-1} \boldsymbol{\Sigma}_{\mathbf{U}_1} (I_{N_1} - A_{11})^{-\top} \bar{\boldsymbol{\tau}}_1). \end{aligned}$$

Indeed, otherwise the KL would not vanish in a neighborhood of non-zero measure and would contradict the fact that \mathcal{L}_{cons} vanishes.

This implies that for all \mathbf{i} in this open neighborhood

$$\bar{\boldsymbol{\tau}}_1^\top (I_{N_1} - A_{11})^{-1}(\boldsymbol{\mu}_{\mathbf{U}_{\pi(1)}} + \mathbf{i}_{\pi(1)}) = \bar{\boldsymbol{\tau}}_1^\top (I_{N_1} - A_{11})^{-1} \boldsymbol{\mu}_{\mathbf{U}_{\pi(1)}} + \boldsymbol{\omega}_1^\top \mathbf{i}_{\pi(1)},$$

which simplifies to

$$\bar{\boldsymbol{\tau}}_1^\top (I_{N_1} - A_{11})^{-1} \mathbf{i}_{\pi(1)} = \boldsymbol{\omega}_1^\top \mathbf{i}_{\pi(1)}.$$

Since this equality between two affine functions of $\mathbf{i}_{\pi(1)}$ is valid on an open set of the vector space of $\mathbf{i}_{\pi(1)}$, these affine functions must be equal (we can reparameterize \mathbf{i} to show that constants must match at the new origin and

the linear maps must match on a basis of the space, so they are equal). This is valid if and only if, in addition to (12), (13),

$$\boldsymbol{\omega}_1 = (I_{N_1} - A_{11})^{-\top} \bar{\boldsymbol{\tau}}_1, \quad (14)$$

is verified.

Alternatively, we obtain the same result by replacing Assum. 3.2 by Assum. B.2. Indeed, as long as the collection of finite interventions vectors forms a rank $\pi(1)$ family, we can choose a subset of $\pi(1)$ such vectors $\{\mathbf{i}_{\pi(1)}^1, \dots, \mathbf{i}_{\pi(1)}^{\pi(1)}\}$ such that it forms a linearly independent family. It can be used to build the matrix equality

$$\bar{\boldsymbol{\tau}}_1^\top (I_{N_1} - A_{11})^{-1} \begin{bmatrix} \mathbf{i}_{\pi(1)}^1, \dots, \mathbf{i}_{\pi(1)}^{\pi(1)} \end{bmatrix} = \boldsymbol{\omega}_1^\top \begin{bmatrix} \mathbf{i}_{\pi(1)}^1, \dots, \mathbf{i}_{\pi(1)}^{\pi(1)} \end{bmatrix} \quad (15)$$

where the matrix $\begin{bmatrix} \mathbf{i}_{\pi(1)}^1, \dots, \mathbf{i}_{\pi(1)}^{\pi(1)} \end{bmatrix}$ is invertible. By right-multiplying Eq. (15) by this inverse, we obtain Eq. (14) again.

We can move on to check the implication of consistency of the effect's conditional. It entails for almost all of \mathbf{i}

$$\widehat{P}^{(\mathbf{i})}(Y|Z)\widehat{P}^{(\mathbf{i})}(Z) = P^{(\omega(\mathbf{i}))}(Y|Z)\widehat{P}^{(\mathbf{i})}(Z) = P^{(0)}(Y|Z)\widehat{P}^{(\mathbf{i})}(Z).$$

The left-hand side is obtained by using

$$(Y, Z) \sim \mathcal{N}(T\boldsymbol{\mu}_X, T\Sigma_X T^\top).$$

And the right-hand side by using

$$Y = f(Z) + R_0.$$

Fitting first only the marginals of Y , we obtain necessary conditions. We have

$$\widehat{P}^{(\mathbf{i})}(Y) = P^{(\omega(\mathbf{i}))}(Y)$$

where for the left-hand side

$$Y = \bar{\boldsymbol{\tau}}_0^\top (I_{N_0} - A_{00})^{-1} \mathbf{U}_{\pi(0)} + \bar{\boldsymbol{\tau}}_0^\top (I_{N_0} - A_{00})^{-1} A_{01} (I_{N_1} - A_{11})^{-1} (\mathbf{U}_{\pi(1)} + \mathbf{i})$$

and for the right-hand side

$$Y \sim f_{\#}[P^{(\omega(\mathbf{i}))}(Z_1)] * P(R_0).$$

As we look for linear Gaussian high-level models, we assume f is affine and parametrize it as $f(Z) = \alpha Z + \beta$. Then, under Assum. 3.2, equality of marginal distributions entails the following equality for all $\mathbf{i}_{\pi(0)}$ in an open neighborhood of 0 (otherwise $\mathcal{L}_{rel} \leq \mathcal{L}_{cons}$ would not vanish)

$$\bar{\boldsymbol{\tau}}_0^\top (I_{N_0} - A_{00})^{-1} \boldsymbol{\mu}_{\mathbf{U}_0} + \bar{\boldsymbol{\tau}}_0^\top (I_{N_0} - A_{00})^{-1} A_{01} (I_{N_1} - A_{11})^{-1} (\boldsymbol{\mu}_{\mathbf{U}_1} + \mathbf{i}_{\pi(1)}) = \alpha \bar{\boldsymbol{\tau}}_1^\top (I_{N_1} - A_{11})^{-1} (\boldsymbol{\mu}_{\mathbf{U}_1} + \mathbf{i}_{\pi(1)}) + \beta + \boldsymbol{\mu}_{R_0}$$

which requires (setting $\mathbf{i} = 0$)

$$+\beta + \boldsymbol{\mu}_{R_0} = \bar{\boldsymbol{\tau}}_0^\top (I_{N_0} - A_{00})^{-1} \boldsymbol{\mu}_{\mathbf{U}_{\pi(0)}}.$$

We can fix $\boldsymbol{\mu}_{R_0}$ to zero to avoid redundancy, such that

$$\boldsymbol{\mu}_{Y|Z=0} = \beta = \bar{\boldsymbol{\tau}}_0^\top (I_{N_0} - A_{00})^{-1} \boldsymbol{\mu}_{\mathbf{U}_{\pi(0)}} \quad (16)$$

and consistency of non-zero shift interventions additionally entail for all \mathbf{i} in the support of $P(\mathbf{i})$

$$\bar{\boldsymbol{\tau}}_0^\top (I_{N_0} - A_{00})^{-1} A_{01} (I_{N_1} - A_{11})^{-1} \mathbf{i}_{\pi(1)} = \alpha \bar{\boldsymbol{\tau}}_1^\top (I_{N_1} - A_{11})^{-1} \mathbf{i}_{\pi(1)}.$$

This yields (since one can always choose a linearly independent family of vectors $\mathbf{i}_{\pi(1)}$ within the open neighborhood of zero for which this equality holds)

$$\bar{\boldsymbol{\tau}}_0^\top (I_{N_0} - A_{00})^{-1} A_{01} (I_{N_1} - A_{11})^{-1} = \alpha \bar{\boldsymbol{\tau}}_1^\top (I_{N_1} - A_{11})^{-1}.$$

Then, right-multiplying by $(I_{N_1} - A_{11})$, we get

$$A_{01}^\top (I_{N_0} - A_{00})^{-\top} \bar{\boldsymbol{\tau}}_0 = \alpha \bar{\boldsymbol{\tau}}_1. \quad (17)$$

Similarly as above, the same conclusion can be drawn if we replace Assum. 3.2 by Assum. B.2.

We can finally check that the conditional distributions are matching. Let us first compute the covariance matrix of the low-level variables.

$$\text{cov}(\mathbf{X}) = \begin{bmatrix} (I_{N_0} - A_{00})^{-1} & (I_{N_0} - A_{00})^{-1}A_{01}(I_{N_1} - A_{11})^{-1} \\ \mathbf{0} & (I_{N_1} - A_{11})^{-1} \end{bmatrix} \Sigma_U \begin{bmatrix} (I_{N_0} - A_{00})^{-\top} & \mathbf{0} \\ (I_{N_1} - A_{11})^{-\top}A_{01}^\top(I_{N_0} - A_{00})^{-\top} & (I_{N_1} - A_{11})^{-\top} \end{bmatrix}.$$

Because the exogenous covariance is diagonal, we get

$$= \begin{bmatrix} (I_{N_0} - A_{00})^{-1}A_{01}(I_{N_1} - A_{11})^{-1}\Sigma_{\pi(1)}(I_{N_1} - A_{11})^{-\top}A_{01}^\top(I_{N_0} - A_{00})^{-\top} & (I_{N_0} - A_{00})^{-1}A_{01}(I_{N_1} - A_{11})^{-1}\Sigma_{\pi(1)}(I_{N_1} - A_{11})^{-\top} \\ + (I_{N_0} - A_{00})^{-1}\Sigma_{\pi(0)}(I_{N_0} - A_{00})^{-\top} & (I_{N_0} - A_{00})^{-1}\Sigma_{\pi(0)}(I_{N_0} - A_{00})^{-\top} \\ \hline (I_{N_1} - A_{11})^{-1}\Sigma_{\pi(1)}(I_{N_1} - A_{11})^{-\top}A_{01}^\top(I_{N_0} - A_{00})^{-\top} & (I_{N_1} - A_{11})^{-1}\Sigma_{\pi(1)}(I_{N_1} - A_{11})^{-\top} \end{bmatrix}.$$

Then,

$$\text{cov}(\widehat{Y}, \widehat{Z}_1) = T \text{cov}(\mathbf{X}) T^\top$$

and

$$\mu_{\widehat{Y}|\widehat{Z}_1} = \mu_{\widehat{Y}} + \bar{\tau}_0^\top (I_{N_0} - A_{00})^{-1} A_{01} (I_{N_1} - A_{11})^{-1} \Sigma_{\pi(1)} (I_{N_1} - A_{11})^{-\top} \bar{\tau}_1 \left(\bar{\tau}_1^\top (I_{N_1} - A_{11})^{-1} \Sigma_{\pi(1)} (I_{N_1} - A_{11})^{-\top} \bar{\tau}_1 \right)^{-1} (\widehat{z}_1 - \mu_{Z_1})$$

Thus using the above equation

$$\mu_{\widehat{Y}|\widehat{Z}_1} = \mu_{\widehat{Y}} + \alpha (\widehat{z}_1 - \mu_{Z_1}) = \bar{\tau}_0^\top (I_{N_0} - A_{00})^{-1} \mu_{U_0} + \bar{\tau}_0^\top (I_{N_0} - A_{00})^{-1} A_{01} (I_{N_1} - A_{11})^{-1} \mu_{\pi(1)} + \alpha \widehat{z}_1 - \alpha \bar{\tau}_1^\top (I_{N_1} - A_{11})^{-1} \mu_{\pi(1)},$$

which further simplifies with the same equation to

$$\mu_{\widehat{Y}|\widehat{Z}_1} = \mu_{\widehat{Y}} + \alpha (\widehat{z}_1 - \mu_{Z_1}) = \bar{\tau}_0^\top (I_{N_0} - A_{00})^{-1} \mu_{U_0} + \alpha \widehat{z}_1.$$

Moreover,

$$\text{var}(\widehat{Y}|\widehat{z}_1) = \sigma_{\widehat{Y}}^2 - \bar{\tau}_0^\top (I_{N_0} - A_{00})^{-1} A_{01} (I_{N_1} - A_{11})^{-1} \Sigma_{\pi(1)} (I_{N_1} - A_{11})^{-\top} \bar{\tau}_1 \left(\bar{\tau}_1^\top (I_{N_1} - A_{11})^{-1} \Sigma_{\pi(1)} (I_{N_1} - A_{11})^{-\top} \bar{\tau}_1 \right)^{-1} \bar{\tau}_1^\top (I_{N_1} - A_{11})^{-1} \Sigma_{\pi(1)} (I_{N_1} - A_{11})^{-\top} A_{01}^\top (I_{N_0} - A_{00})^{-\top} \bar{\tau}_0$$

again, using the above equation this leads to the simplification

$$\begin{aligned} \text{var}(\widehat{Y}|\widehat{z}_1) &= \sigma_{\widehat{Y}}^2 - \alpha \bar{\tau}_1^\top (I_{N_1} - A_{11})^{-1} \Sigma_{\pi(1)} (I_{N_1} - A_{11})^{-\top} A_{01}^\top (I_{N_0} - A_{00})^{-\top} \bar{\tau}_0 \\ &= \sigma_{\widehat{Y}}^2 - \alpha \bar{\tau}_1^\top (I_{N_1} - A_{11})^{-1} \Sigma_{\pi(1)} (I_{N_1} - A_{11})^{-\top} \bar{\tau}_1 \alpha \\ &= \bar{\tau}_0^\top (I_{N_0} - A_{00})^{-1} \Sigma_{\pi(0)} (I_{N_0} - A_{00})^{-\top} \bar{\tau}_0. \end{aligned}$$

For the high-level distribution we get

$$P(Y|z) = \mathcal{N}(\alpha z + \beta, \sigma_Y^2)$$

where we can identify all parameters with the above equations. □

B.3 Proof of Proposition 3.4

Proposition 3.4. *Consider the setting of Prop. 3.3 with the exception that $\Omega \subsetneq \pi(1)$ such that there is now a non-empty subset $S = \pi(1) \setminus \Omega$, such that $\mathbf{X}_\Omega \rightarrow \mathbf{X}_S \rightarrow \mathbf{X}_{\pi(0)}$. Then there exist at least two different linear 1D TCR such that $\mathcal{L}_{\text{cons}} = 0$.*

Proof. The low-level model follows the following SCM, with $P(\mathbf{i})$ non-trivial

$$\mathbf{X} := \mathbf{A}\mathbf{X} + \mathbf{U} + \mathbf{i}, \quad U_k \sim \mathcal{N}(\mu_k, \sigma_k^2)$$

such that \mathbf{X} , A and P take the block forms

$$\mathbf{X} = \begin{bmatrix} \mathbf{X}_{\pi(0)} \\ \mathbf{X}_S \\ \mathbf{X}_\Omega \end{bmatrix}, \quad A = \begin{bmatrix} A_{00} & A_{0S} & \mathbf{0} \\ \mathbf{0} & A_{SS} & A_{S\Omega} \\ \mathbf{0} & \mathbf{0} & A_{\Omega\Omega} \end{bmatrix},$$

with $\pi(0)$ of size N_0 , and $\pi(1)$ of size $N_1 = N - N_0$ and S of size s . Then we know from the Proposition 3.3 that there is already a valid solution using π as alignment. The only difference is that variables in S are unintervened, which does not affect the ability of the solution to achieve $\mathcal{L}_{cons} = 0$. That solution would be compatible with interventions on S , but since S is unintervened, we do not have uniqueness guarantees for this choice of π .

Alternatively, if we choose $\pi'(0) = \pi(0) \cup S$ and $\pi'(1) = \pi(1) \setminus S = \Omega$, then, we can again apply Proposition 3.4, and see that it provides a different solution with this alignment, which is compatible with the given problem (constructive transformation with constraint on the mapping τ_0). Importantly, the key indeterminacy is for the map τ_1 , which will either put all its weight on elements in S (direct parents of $\pi(0)$), or alternatively, put all its weights on elements in Ω . There is an additional, but trivial, indeterminacy for the map ω_1 : indeed, since X_S is unintervened (as part of $\pi(0)$), the weights in ω_1 associated to these coefficients may take arbitrary values (since their associated component in \mathbf{i} remains zero). We do not consider these trivial indeterminacies (which do not affect the mapping ω_1 on its domain, i.e. the support of the prior $P(\mathbf{i})$) by forcing the weights of ω_1 associated to unintervened variables to zero. \square

C THE CASE $n > 1$: MULTIPLE HIGH-LEVEL CAUSES

C.1 Updated setting

We generalize the main text setting of the linear reduction framework to learn $n > 1$ high-level causes as follows.

Tau map The τ -map now incorporates $n + 1$ components, associated to each cause and to Y , respectively.

$$\mathbf{X} \mapsto \begin{bmatrix} Y \\ \mathbf{Z} \end{bmatrix} = \begin{bmatrix} \tau_0(\mathbf{X}_{\pi(0)}) \\ T\mathbf{X} \end{bmatrix} = [\tau_0^\top \mathbf{X}_{\pi(0)} \quad \tau_1^\top \mathbf{X}_{\pi(1)} \quad \dots \quad \tau_n^\top \mathbf{X}_{\pi(n)}]^\top$$

Omega map We define the collection of n vectors $\{\omega_k\}$ associated to interventions on each high-level cause. Again, no intervention is performed on the target Y .

$$\omega(\mathbf{i}) = W\mathbf{i} = [\omega_1^\top \mathbf{i}, \dots, \omega_n^\top \mathbf{i}]^\top = [\bar{\omega}_1^\top \mathbf{i}_{\pi(1)}, \dots, \bar{\omega}_n^\top \mathbf{i}_{\pi(n)}]^\top,$$

High-level mechanisms As illustrated by Fig.1b, we now have n causes are root nodes, which implies that the high-level model represents their mechanism as sampling from independent scalar exogenous variables. In the Gaussian case, this entails modeling their joint distribution by a multivariate Gaussian with diagonal covariance. The additional mechanism, associated with Y , is now a function f_Y that simply takes multiples causes as input, in addition to its independent exogenous variable R_0 . In the linear Gaussian SCM case, this is simply implemented by applying multiplicative coefficients to each input and summing the outcome.

C.2 Additional indeterminacies and group sparsity loss

In the $n = 1$ high-level cause setting, choosing $\pi(1)$ is unproblematic, as one can just select variables relevant for interpretability among all components of \mathbf{X} that are not used to compute Y . In contrast, for $n > 1$ causes, the choice of the subsets $\pi(1), \dots, \pi(n)$ is non-trivial. One the one-hand, being strict about imposing constructive transformations would entail that those subsets do not have any pairwise overlap. On the other hand, causes “compete” to account for the interventional changes in Y , which may lead them to put large weights on the same variables in their vectors τ_k and ω_k . Additionally, there is nothing in the consistency loss preventing one single cause, say Z_1 , taking over all the causal explanation of Y , while the other high-level causes Z_2, \dots, Z_n may just be chosen as irrelevant variables independent of (and having no influence on) Y .

In order to prevent a single cause taking over and softly enforce that each of them focus on different subsets of low-level variables, we take inspiration from losses enforcing structured sparsity (Jenatton et al., 2011). We

assume that domain-knowledge can inform us about subsets of low-level variables, preferably belong to the same subset $\pi(k)$. The idea behind is to group variables of the same nature, pertaining to the same mechanism, or associated to neighboring location in the coordinate system. In this way, the cause Z_k associated to subset $\pi(k)$ may be interpreted as conveying information about an interpretable aspect of the model. Let $G_1, \dots, G_M \subseteq [1..N]$ define such groups of low-level variables. Then, we define the group sparsity loss as

$$\sum_{j=1}^n \frac{\left(\sum_{m=1}^M \sqrt{\sum_{k \in G_m} (\tau_j)_k^2} \right)^2}{\sum_{m=1}^M \sum_{k \in G_m} (\tau_j)_k^2} - n. \quad (18)$$

While the numerator corresponds to the family of convex group sparsity inducing losses (Jenatton et al., 2011), we adapt it to our setting by normalizing it by an ℓ_2 squared norm at the numerator in order to make this loss invariant by multiplicative rescaling of the τ_k vectors. This avoids the algorithm to downscale the reduction map. This regularization encourages the different high-level variables to focus on different groups of nodes and is a way to encode prior knowledge about the system in the TCR. The use of this loss is exemplified in App. F.2 and Fig. 9.

D ADDITIONAL THEORY

D.1 Reparametrizations of reductions

In order to study invariance properties of TCR, we define transformations compatible with a class of reductions. Let $\rho : \mathcal{Z}_1 \times \dots \times \mathcal{Z}_n \rightarrow \mathcal{Z}_1 \times \dots \times \mathcal{Z}_n$ be a continuous invertible transformation of the n -dimensional high-level cause vector. Then the transformation

$$\tilde{\rho} : \begin{bmatrix} Y \\ \mathbf{Z} \end{bmatrix} \mapsto \begin{bmatrix} Y \\ \rho(\mathbf{Z}) \end{bmatrix}$$

is also continuous invertible. Among this class of transformations, we define an invertible reparametrization of a TCR as follows.

Definition D.1. *An invertible reparametrization of a reduction for the class \mathcal{T} of τ -maps and the class $\{\mathcal{H}_\gamma\}_{\gamma \in \Gamma}$ satisfies the following properties.*

- it is compatible with the class of τ -maps as follows: for any map $\tau \in \mathcal{T}$, we have $\tilde{\rho} \circ \tau \in \mathcal{T}$,
- it is compatible with the high-level model class $\{\mathcal{H}_\gamma\}$ as follows: for any model parameter γ , the unintervened and intervened distributions $P_{\mathcal{H},\gamma}(Y, \mathbf{Z})$ are such that there exist a parameter γ' and a map between high-level interventions $\psi : \mathcal{J} \rightarrow \mathcal{J}$ such that the joint distributions of the transformed variables $(Y, \rho(\mathbf{Z}))$ is compatible with unintervened and intervened distributions of $\mathcal{H}_{\gamma'}$, in the sense that

$$\tilde{\rho}_\# [P_{\mathcal{H},\gamma}^{(j)}(Y, \mathbf{Z})] = P_{\mathcal{H},\gamma'}^{(\psi(j))}(Y, \mathbf{Z}).$$

D.2 The case of a single target low-level variable

Whenever $\pi(0)$ is a singleton, τ_0 is univariate and the target Y essentially corresponds (up to trivial rescaling) to a single low-level variable. We elaborate on the interpretation of Proposition 3.3 in this context.

Let us set $\bar{\tau}_0 = 1$ and fix the target index such that $\pi(0) = \{N\}$ without loss of generality. Then the DAG constraints entail $A_{00} = 0$ and the structural equations take the form

$$\mathbf{X}_{\pi(1)} := A_{11} \mathbf{X}_{\pi(1)} + \mathbf{U}_{\pi(1)} + \mathbf{i}, \quad U_k \sim \mathcal{N}(\mu_k, \sigma_k^2) \quad (19)$$

$$Y := \mathbf{a}_{01}^\top \mathbf{X}_{\pi(1)} + U_N \quad (20)$$

where \mathbf{a}_{01} is a column vector of coefficients of the low-level mechanism linking the target Y to its causes in $\pi(0)$. Then the unique linear 1D TCR, up to a multiplicative constant, making the consistency loss vanish is given by

$$\bar{\tau}_1 = \mathbf{a}_{01} \quad (21)$$

$$\text{and } \bar{\omega}_1 = (I_{N-1} - A_{11})^{-\top} \bar{\tau}_1 = (I_{N-1} - A_{11})^{-\top} \mathbf{a}_{01}. \quad (22)$$

This solution is easily interpretable: $\bar{\tau}_1$ identifies the ground truth mechanism linking $\mathbf{X}_{\pi(0)}$ to the target, while $\bar{\omega}_1$ traces the contribution of interventions on each endogenous variable to the target. Indeed, this contribution is given by the “reduced form” map between exogenous values and endogenous values (see proof of Proposition 3.3 for more insights)

$$\mathbf{i} \mapsto (I_{N-1} - A_{11})^{-1} \mathbf{i},$$

and by composing this mapping with mechanism \mathbf{a}_{01} we get the (shift) influence of interventions on the target

$$\mathbf{i} \mapsto \mathbf{a}_{01}^\top (I_{N-1} - A_{11})^{-1} \mathbf{i} = \bar{\omega}_1^\top \mathbf{i}.$$

The mismatch between $\bar{\omega}_1$ and $\bar{\tau}_1$ is due to the internal causal structure of the submodel described by eq. (19). Indeed, if there are no causal links within this subsystem, A_{11} is a zeros matrix and

$$\bar{\omega}_1 = (I_{N-1})^{-\top} \bar{\tau}_1 = \bar{\tau}_1 = \mathbf{a}_{01},$$

otherwise, the two maps will be different. The discrepancy between the vectors thus reflects the fact that the causal explanation links high-level endogenous variables and interventions on them by potentially complex low-level interactions that do not necessarily have a simple high-level interpretation. This justifies regularizing the consistency loss with an homogeneity loss in order to focus on explanations that exhibit congruent τ and ω maps.

D.3 The case of linear chain SCMs

In the case of a chain SCM

$$\mathbf{X}_1 \rightarrow \dots \rightarrow \mathbf{X}_{N-1} \rightarrow \mathbf{X}_N = Y$$

the above linear setting gets the additional constraints (using a causal ordering of the variables) that the target’s mechanism is sparse

$$\mathbf{a}_{01}^\top = [0, \dots, 0, a_N]$$

and the structure matrix of $\mathbf{X}_{\pi(1)}$ is subdiagonal

$$A_{11} = \begin{bmatrix} 0 & 0 & \dots & 0 & 0 \\ a_2 & 0 & \dots & 0 & 0 \\ 0 & a_3 & \dots & 0 & 0 \\ 0 & 0 & \dots & 0 & 0 \\ 0 & 0 & \dots & a_{N-1} & 0 \end{bmatrix}$$

and as a consequence, the solution writes

$$\bar{\tau}_1 = [0, \dots, 0, a_{N-1}]^\top \quad (23)$$

$$\text{and } \bar{\omega}_1 = (I_{N-1} - A_{11})^{-\top} \bar{\tau}_1 = \begin{bmatrix} a_2 \cdot a_3 \cdot \dots \cdot a_{N-1} \\ \vdots \\ a_{N-2} a_{N-1} \\ a_{N-1} \end{bmatrix}. \quad (24)$$

This solution is in line with our experimental results:

- $\bar{\tau}_1$ has all its weight on the parent of the target.
- $\bar{\omega}_1$ has a non-sparse distribution over the chains, decaying in the upstream direction. This reflects that structure coefficients of A_{11} are selected with absolute value inferior to one, such that the influence of ancestor nodes on the target decays with their distance to it on the graph.

Transposing the chain example to the case of Proposition 3.4, we can take the case were the direct parent X_{N-1} of the target is left unintervened. In such a case, $\bar{\tau}_1$ may put its weight on both X_{N-1} and its direct parent X_{N-2} , Proposition 3.3 provides two example solutions for different choices of $\pi(1)$, including or excluding X_{N-1} . In the most extreme case of dissimilarity between τ_1 and ω_1 , solution including X_{N-1} in $\pi(1)$ puts all τ_1 ’s weight on X_{N-1} , while ω_1 has no weight on it (because it is unintervened). As a consequence, ω_1 and τ_1 are orthogonal and the associated homogeneity loss vanishes. In contrast, the unique solution excluding X_{N-1} from $\pi(1)$ have a larger cosine similarity and will thus be preferred by the homogeneity-regularized loss.

E ALGORITHM DETAILS

E.1 Gaussian consistency loss

As the KL divergence is hard to estimate in the non-parametric setting, we make a Gaussian approximation of this loss to get an analytical, differentiable expression. Using the general formula for two n-dimensional Gaussian densities P and Q

$$KL(P||Q) = \frac{1}{2} \left[(\mu_Q - \mu_P)^\top \Sigma_Q^{-1} (\mu_Q - \mu_P) + \text{tr}(\Sigma_Q^{-1} \Sigma_P) - \log \frac{|\Sigma_P|}{|\Sigma_Q|} - n \right].$$

Parameters of the reduction are $\tau_k, \mu_Z, \mu_{Y|Z}, f : z \rightarrow f(z), \omega_k$ with

$$\begin{aligned} Z^{(\omega^{(i)})} &\sim P(z) = \mathcal{N}(\mu_Z + Wi, \Sigma_Z, \text{ with } W = [\omega_1, \dots, \omega_n]^\top \text{ and } \Sigma_Z = \text{diag}(\sigma_{Z,1}^2, \dots, \sigma_{Z,n}^2)) \\ Y^{(\omega^{(i)})}|z &\sim P(Y|z) = \mathcal{N}(f(z), \sigma_{Y|Z}^2), \\ \hat{Z}^{(i)} &= [\tau_1, \dots, \tau_n]^\top X^{(i)} = T X^{(i)}, \\ \hat{Y}^{(i)} &= \tau_0^\top X^{(i)}. \end{aligned}$$

Moreover, we estimate the second order properties of the simulator distribution for each intervention i

$$\begin{aligned} \hat{\mu}_X^{(i)} &= \langle X^{(i)} \rangle, \\ \hat{\Sigma}_X^{(i)} &= \left\langle \left(X^{(i)} - \hat{\mu}_X^{(i)} \right)^\top \left(X^{(i)} - \hat{\mu}_X^{(i)} \right) \right\rangle, \\ \hat{\mu}_Z^{(i)} &= \langle \hat{Z}^{(i)} \rangle = T \hat{\mu}_X^{(i)}, \\ \hat{\mu}_Y^{(i)} &= \langle \hat{Y}^{(i)} \rangle = \tau_0^\top \hat{\mu}_X^{(i)}, \\ \hat{\Sigma}_Z^{(i)} &= \left\langle \left(\hat{Z}^{(i)} - \hat{\mu}_Z^{(i)} \right) \left(\hat{Z}^{(i)} - \hat{\mu}_Z^{(i)} \right)^\top \right\rangle = T \hat{\Sigma}_X^{(i)} T^\top, \\ \widehat{\sigma}_{Z,k}^{(i)} &= \left(\hat{\Sigma}_Z^{(i)} \right)_{k,k} = \left\langle \left(\hat{Z}_k^{(i)} - \hat{\mu}_{Z,k}^{(i)} \right)^2 \right\rangle = \tau_k^\top \hat{\Sigma}_X^{(i)} \tau_k, \\ \widehat{\sigma}_Y^{(i)} &= \left\langle \left(\hat{Y}^{(i)} - \hat{\mu}_Y^{(i)} \right)^2 \right\rangle = \tau_0^\top \hat{\Sigma}_X^{(i)} \tau_0, \\ \widehat{c}_{ZY}^{(i)} &= \left\langle \left(\hat{Y}^{(i)} - \hat{\mu}_Y^{(i)} \right) \left(\hat{Z}^{(i)} - \hat{\mu}_Z^{(i)} \right) \right\rangle = T \hat{\Sigma}_X^{(i)} \tau_0, \end{aligned}$$

where $\langle \cdot \rangle$ denotes the empirical average. Using the KL between Gaussian variables, we can rewrite the consistency loss as

$$\begin{aligned} \mathcal{L}_{cons} &= \mathbb{E}_{i \sim p(i)} \left[KL_z(\hat{P}^{(i)}(z) | P(\hat{\omega}^{(i)}(z))) \right] + \mathbb{E}_{z \sim \hat{P}^{(i)}(Z)} \left[KL_Y(\hat{P}^{(i)}(Y|Z=z) || P^{(0)}(Y|Z=z)) \right] \\ &= \frac{1}{2} \mathbb{E}_{i \sim p(i)} \left[\sum_k \left(\frac{(\mu_{Z,k} + \omega_k^\top i - \hat{\mu}_{Z,k}^{(i)})^2}{\sigma_{Z,k}^2} + \frac{\widehat{\sigma}_{Z,k}^{(i)}}{\sigma_{Z,k}^2} \right) - \ln \left(\frac{|\hat{\Sigma}_Z^{(i)}|}{\prod_k \sigma_{Z,k}^2} \right) - n \right] \\ &\quad + \frac{1}{2} \mathbb{E}_{i \sim p(i), z \sim \hat{P}^{(i)}(Z)} \left[\frac{\left(f(z) - \hat{\mu}_Y^{(i)} - \left(\widehat{c}_{ZY}^{(i)} \right)^\top \left(\hat{\Sigma}_Z^{(i)} \right)^{-1} (z - \hat{\mu}_Z^{(i)}) \right)^2}{\sigma_{Y|Z}^2} \right. \\ &\quad \left. + \frac{\widehat{\sigma}_Y^{(i)} - \left(\widehat{c}_{ZY}^{(i)} \right)^\top \left(\hat{\Sigma}_Z^{(i)} \right)^{-1} \widehat{c}_{ZY}^{(i)}}{\sigma_{Y|Z}^2} - \ln \left(\frac{\widehat{\sigma}_Y^{(i)} - \left(\widehat{c}_{ZY}^{(i)} \right)^\top \left(\hat{\Sigma}_Z^{(i)} \right)^{-1} \widehat{c}_{ZY}^{(i)}}{\sigma_{Y|Z}^2} \right) - 1 \right]. \quad (25) \end{aligned}$$

The overall algorithm is described in the Algorithm 1 of main text.

F EXPERIMENTAL DETAILS

F.1 Experimental settings

Sampling linear Gaussian low-level models For the adjacency matrix, we sample all non-zero entries uniformly in the interval $[-1, 1]$. For general adjacency matrices, the lower triangular elements of the adjacency matrix are non-zero, where we assume that the target Y has only incoming edges and the variables are arranged in topological order. For chain graphs, the first lower off-diagonal entries are non-zero. The exogenous variables U and shift interventions \mathbf{i} are independent Gaussian with $U_j, i_j \sim \mathcal{N}(0, 1)$ for $j = 1, \dots, n$.

Double well We model the ball moving in a double well potential $V(x) = x^4 - 4x^2$, shown in Figure 5(a), by the following equation of motion:

$$m\ddot{x}(t) + k\dot{x}(t) + \frac{\partial}{\partial x}V(x(t)) = 0 \quad \Rightarrow \quad m\ddot{x}(t) + k\dot{x}(t) + 4x(t)^3 - 8x(t) = 0, \quad (26)$$

where $x(t)$ is the position of the ball at time t , $\dot{x}(t)$ and $\ddot{x}(t)$ are the first and second time derivatives, respectively, k is the friction coefficient and m is the mass of the ball. We can reformulate the second order ODE into a system of first order ODEs by introducing the velocity $v(t) = \dot{x}(t)$ as a variable:

$$\begin{aligned} \dot{x}(t) &= v(t) \\ \dot{v}(t) &= -\frac{1}{m} \left(kv(t) + 4x(t)^3 - 8x(t) \right). \end{aligned} \quad (27)$$

We solve the system of ODEs numerically on a grid of 101 time points t_k for $k = 0, \dots, 100$ equally spaced between $t = 0$ and $t = 40$ using a numerical integration method. The initial conditions are $x(0) = -2.07414285 + 5 \times 10^{-7} \times \varepsilon_x$, with $\varepsilon_x \sim \text{Uniform}(-1, 1)$ and $v(0) = 11$. The initial values are chosen such that there is a non-zero chance that the ball ends up in the left or right well without any additional interventions.

For shift interventions, we sample random velocity shifts $\Delta v(t_k) \sim \mathcal{N}(0, 0.5)$. The positions are unshifted. In the numerical integration scheme, the shift interventions are implemented by splitting the integration domain in parts. The ODE system is integrated from the initial conditions at t_0 to the next time grid at t_1 . Then the velocity at t_1 is shifted by $\Delta v(t_1)$ and used as the initial value for the next integration starting at t_1 , and so on. Similarly, we introduce independent stochasticity by adding noise to the velocity sampled from $\mathcal{N}(0, 0.2)$ at each time step, mimicking intrinsic noise of the system.

F.2 Additional results

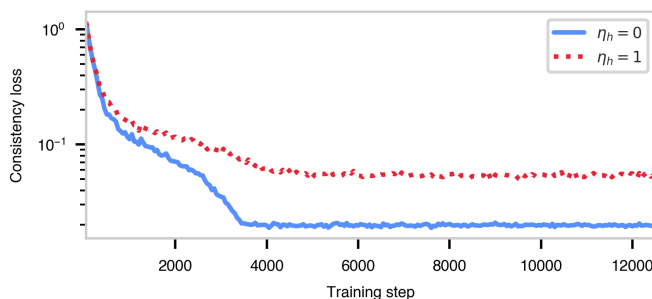


Figure 6: **Comparison of consistency loss during training for chain graphs with and without homogeneity regularization.** The training consistency loss, averaged over 20 runs, is shown for two regularization settings. Similarly, we depict the normalized ω_1 parameters. We compare two training settings: with and without homogeneity regularization (9) ($\eta_h = 0$ or $\eta_h = 1$, respectively). Each run corresponds to a draw of the adjacency parameters.

Linear chain As hinted at in Section 5.1, adding homogeneity regularization (9), while promoting interpretability, comes at the cost of a worse consistency of the high-level abstraction, which is shown in Figure 6.

Double well As shown in Figure 7, introducing homogeneity regularization (9) aligns the τ - and ω maps, while still capturing the correct system dynamics. In Figure 8, during training the total loss and its consistency and homogeneity contributions converge.

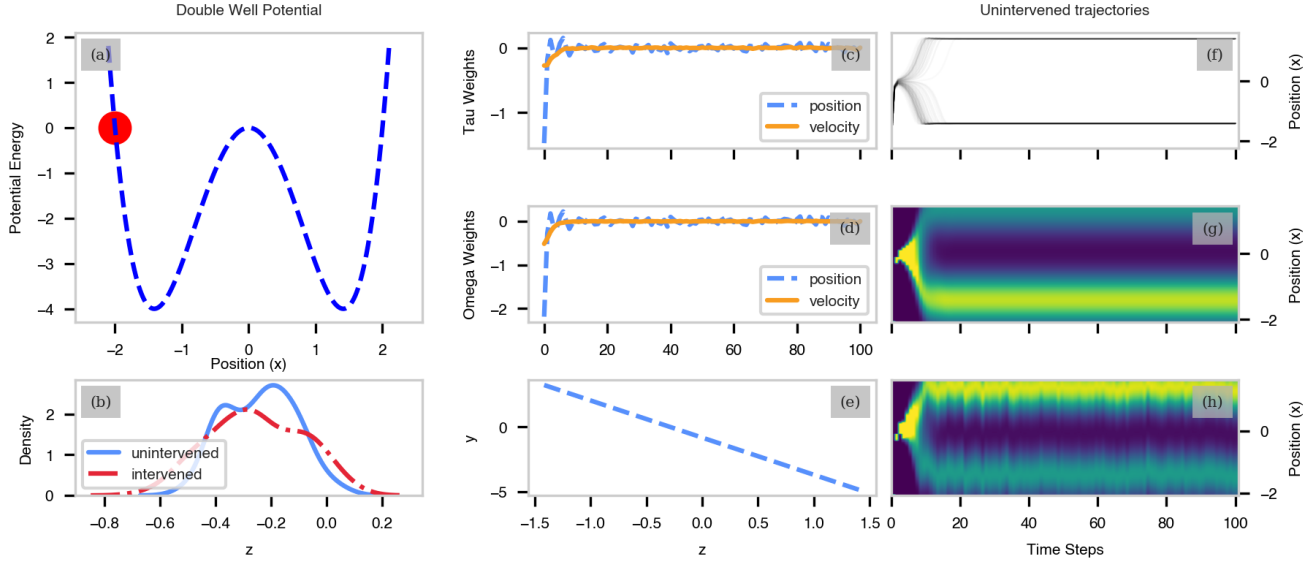


Figure 7: **Double well experiment with homogeneity regularisation** ($\eta_h = 1$). Comparison of samples and inferred causal factors in the double well experiment. (a) Depicts the experimental setup with a ball moving in a double well potential subject to linear friction. (b) Displays the pushforward density of the high-level cause for the two settings: one where no intervention is applied (unintervened), and the other with an applied shift intervention. (c) and (d) represent the learned parameters, τ and ω , respectively. (e) Illustrates the conditional mean $\mathbb{E}[Y | Z]$ for the inferred high-level causal mechanism. (f) and (g) show samples from the unintervened setting and the corresponding estimated density. (h) Depicts the estimated density for the intervened setting.

Two branch linear graph In order to test the linear TCR algorithm 1 for multiple high-level causes, we sample from a linear Gaussian low-level model with a graph with two branches $X_1 \rightarrow X_2 \rightarrow X_3 \rightarrow X_4 \rightarrow X_{10} \leftarrow X_9 \leftarrow \dots \leftarrow X_5$. Here, X_{10} is the target variable. We train a two-cause TCR and use the two branches as groups for the group sparsity regularization (18): $G_1 = \{1, \dots, 4\}$ and $G_2 = \{5, \dots, 9\}$. The trained τ - and ω parameters are shown in Figure 9. We observe that the regularization, together with the prior information on the relevant variable groups, correctly guides TCR to identify the two branches as the high-level causes of the target X_{10} , where τ_1 and ω_1 summarize the first branch $X_1 \rightarrow \dots \rightarrow X_4$, whereas τ_2 and ω_2 focus on the branch $X_5 \rightarrow \dots \rightarrow X_9$.

F.3 Training parameters and computing resources

For TCR training, we use the ADAM optimizer and train on NVIDIA RTX-6000 GPUs on our internal cluster. The other training parameters are summarized in Table 1. The parameters were chosen manually to ensure the training loss converges.

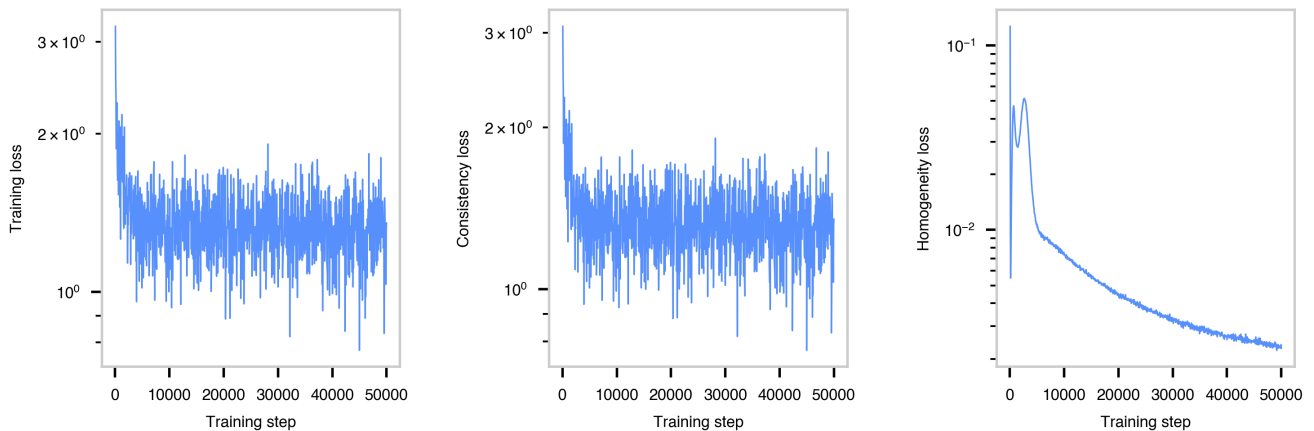


Figure 8: **Double well training** ($\eta_h = 1$).

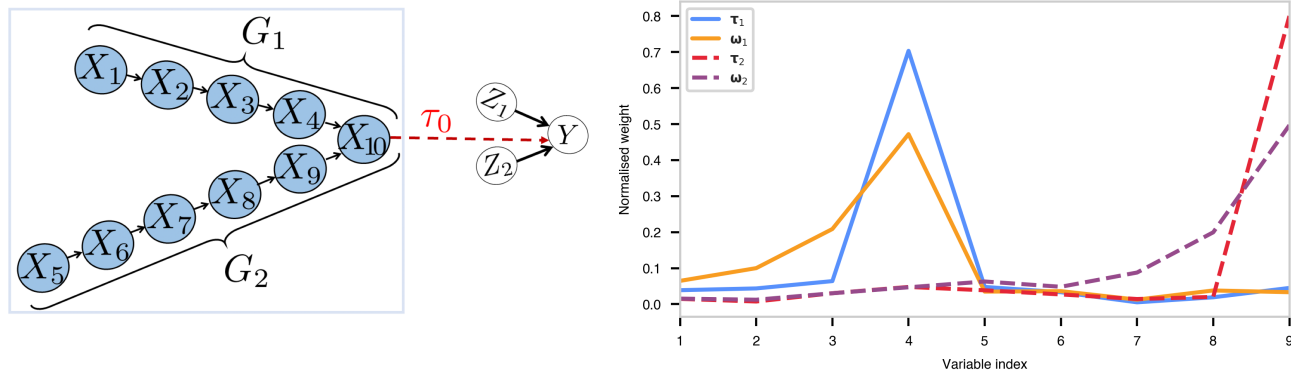


Figure 9: **Comparison of learned τ - and ω parameters for the two branch graph and a two-cause TCR.** The two-branch, low-level graph, the variable groups for the group sparsity regularization and high-level causal model are shown on the left. The normalized τ_i parameters, shown on the right, $((\tau_i)_k / \sum_{k'} (\tau_i)_{k'})$, where k corresponds to the low-level variable index for $i = 1, 2$ are averaged over 20 runs. Each run corresponds to a draw of the adjacency parameters. Similarly, we depict the normalized ω parameters.

Parameters	Linear	Double Well
learning rate λ	0.001	0.001
simulation paths n_{sim}	10,000	10,000
training epochs N_{ite}	100	100-400
simulation batch size B	128	128
intervention batch size B_i	64	64

Table 1: **Experimental parameters and settings**